

ESTIMATION AND ANALYSIS OF HARMONICS IN POWER SYSTEM

A DISSERTATION

Submitted in partial fulfilment of the requirements for the award of the degree

of

MASTER OF ENGINEERING

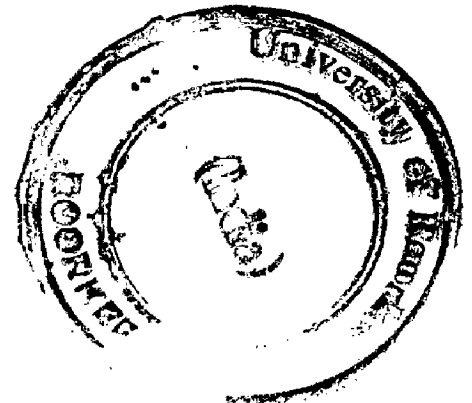
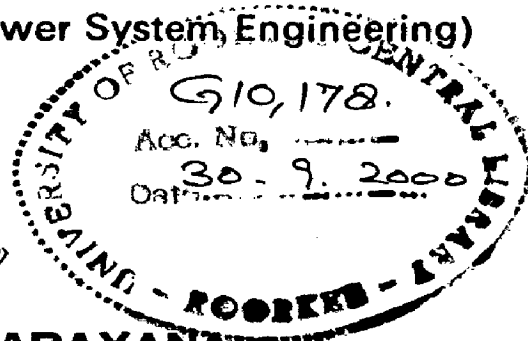
in

ELECTRICAL ENGINEERING

(With Specialization in Power System Engineering)

By

S. SIVANNARAYANA



**DEPARTMENT OF ELECTRICAL ENGINEERING
UNIVERSITY OF ROORKEE
ROORKEE-247 667 (INDIA)**

MARCH, 2000

10/03/2000

CANDIDATE'S DECLARATION

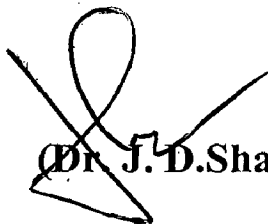
I hereby declare that the work presented in this dissertation entitled **“ESTIMATION AND ANALYSIS OF HARMONICS IN POWER SYSTEM”**, submitted in partial fulfillment of the requirement for the award of the degree of **Master of Engineering, in Electrical Engineering**, with specialization in **Power System Engineering**, in the Department of Electrical Engineering, University of Roorkee, Roorkee, is an authentic record of my own work, carried out with effect from July 1999 to March 2000, under the guidance of **Dr. J . D. Sharma** and, **Dr. B. Das** Department of Electrical Engineering, University of Roorkee, Roorkee.

The matter embodied in this thesis has not been submitted for the award of any other degree.

DATE : 31 March, 2000.

S. Sivannarayana
(S. SIVANNARAYANA)

It is certified that the above statement made by the candidate is correct to the best of our knowledge and belief.


(Dr. J. D. Sharma)

Biswamp Das
31.3.2000
(Dr. B. Das)

Department of Electrical Engineering
University of Roorkee
Roorkee – 247667
(INDIA)

ACKNOWLEDGEMENT

I would like to express my deep sense of gratitude to my guides **Dr. J.D. Sharma**, professor, and **Dr. B.Das**, Lecturer, Department of electrical engineering, University of Roorkee, Roorkee, for their invaluable guidance, unfailing inspiration, whole hearted co-operation and generous help in carrying out this work. Their encouragement at each step of the work and pain-staking efforts in providing valuable suggestions are greatly acknowledged.

Thanks are due to Dr. Bharat Gupta, o.c. power system simulation lab for providing and extending all the facilities.

I cannot forget to recall, with my heartiest regards, the ever ending heart felt stream of caring and tender love which my respected parents bestowed upon me. It was the power of their blessings, which gave me courage and confidence to materialize my dreams.

At last but not least, thanks to all those who have directly or indirectly helped me at any stage of my work.

S. Sivannarayana
(S.SIVANNARAYANA)

ABSTRACT

A rapid increase in harmonic currents and voltages in the present AC systems due to large introduction of solid state switching devices. It is imperative to know the harmonic parameters such as magnitude and phase angles. This is essential for designing filters for eliminating and reducing the effects of harmonics in a power system.

In the present work, An artificial neural network based approach has been presented to estimate the harmonic source currents injected into the system. Three-layered feed forward structured neural network was constructed with backpropagation learning algorithm. Neural network was trained and tested with the 18-bus example system, the results obtained from the tests showed acceptable estimates.

NOMENCLATURE

a	Fourier coefficient
$A^{(m)}, B^{(m)}$	Constants in m^{th} solution region
B	Phase angle
c	Fourier coefficient
C	Constant
D	Distortion Volt amps
g_i, g_r	Imaginary and real parts of current balance equation
H	Harmonic jacobian entry
h,n	Number of harmonics considered
I_i, I_r	Imaginary and real parts of i^{th} harmonic current
$J^l, J^{(i)}$	Convension and harmonic Jacobian matrix
k	Harmonic number
K	Constant
ΔM	Mismatch vector
n	Number of system buses
N	Number of non-linear loads
$P^{(m)}$	Inverse time constant, m^{th} solution region
T	Time
ΔU	Voltage correction
ΔW	Mismatch P,Q
Y_k	Entries in harmonic jacobian
δ_k	Triad
ω_0	Fundamental frequency
u_a, u_b, u_c	Phase to neutral voltages
N_j	Jacobian dimension
N_j	Number of non-zero entries in jacobian
t(superscript)	Transpose
$\Delta v, \Delta \alpha$	Update on v, α
$\theta^{(i)}, \phi^k$	Phase angle of i^{th} harmonic voltage

CONTENTS

	<i>page</i>
CANDIDATE'S DECLARATION	i
ACKNOWLEDGEMENT	ii
ABSTRACT	iii
NOMENCLATURE	iv
LIST OF FIGURES	vii
LIST OF TABLES	viii
CHAPTER 1 INTRODUCTION	1
1.1 Introduction	1
1.2 State-of-art	2
1.2.1 Mathematical models for harmonic power flow	3
1.2.2 Harmonic power flow methods	4
1.2.3 Artificial neural networks	5
1.3 Objectives of present study	6
1.4 Organization of dissertation	6
CHAPTER 2 HARMONIC POWER FLOW ANALYSIS	7
2.1 Definitions related to harmonics	7
2.2 Modeling of network components	8
2.2.1 Transmission line model	8
2.2.2 Synchronous machine model	10
2.2.3 Load models	11
2.2.4 Modeling of other network elements	11
2.2.5 Non-linear resistive load model	12
2.2.6 Modeling of converter	13
2.3 Newton-Raphson method for harmonic load flow analysis	16
2.4 Flowchart for harmonic power flow	21
2.5 Sparsity programming method for the harmonic power flow	21

CHAPTER 3	FEED FORWARD NEURAL NETWORKS	24
3.1	Introduction to ANN	24
3.2	Feed forward backpropagation network	25
3.2.1	Architecture of the ANN	25
3.2.2	Error minimization and weight change Computation	27
3.3	Stepwise solution algorithm	28
3.4	Flowchart for training of backpropagation algorithm	30
CHAPTER 4	RESULTS AND DISCUSSION	31
4.1	Neural network training process	31
4.2	Training of 18 bus system	32
CHAPTER 5	CONCLUSIONS AND SCOPE FOR FUTURE WORK	35
	REFERENCES	36
	APPENDIX A	39
	APPENDIX B	41

LIST OF FIGURES

FIG .NO.	CAPTION	PAGE NO
2.1	Equivalent PI representation of long transmission line	9
2.2	Power flow model of synchronous machine	10
2.3	Power flow model of Generalized conventional load	11
2.4	full wave six pulse bridge rectifier	14
2.5	Sparsity storage technique using LLT/URT storage and chained data	23
3.1	three layer feed forward neural network	26
3.2	A basic processing unit	26
4.1	Structured neural network	32
4.2	18 bus example system	33

Chapter 1

Introduction

1.1 INTRODUCTION

Estimation of harmonic components in a power system is a standard approach for the assessment of the quality of the delivered power. Power system harmonics are known to be generated by a number of sources in the power network. The use of alternating current circuits in electrical power system has been common place nearly since the very inception of the interconnected power network. The most familiar loads on such a system are the constant power, constant impedance and constant current loads or a linear combination of thereof. In typical cases, the voltage and current waveshapes are nearly purely sinusoidal. In a modern electric power system loads may occur in which voltage or current waveforms are distorted. Prior to the development of static converter plant power system harmonic distortion was primarily with the design and operation of electric machines and transformers. Indeed the principal harmonic source present in the system in early days was the magnetising current of transformers, electrical generators provided the main secondary source. Since this practical economic design required that some departure from the ideal sinusoidal waveshapes be accepted, often harmonic signal levels on early power system could be reduced to acceptable levels through the use of wye-delta transformers. Today, the number and significance of harmonic producing elements is rapidly increased due to the development of high power semiconductor switches and the widespread use of fluorescent lighting. Because of the absence of stability problem and certain other advantages of low loss and efficient use of right-of-way, HVDC subsystem takes an important role in long distance transmission. In recent years, the HVDC conversion technique has been perfected and HVDC transmission has been applied in several countries of the world. Unfortunately, the character of HVDC converter is non-linear and the converter is a harmonic source in the power system.

Gaseous discharge lighting (such as fluorescent, mercury arc and high pressure sodium) is a significant source of power system harmonics, particularly in metropolitan

areas. The electrical characteristics of this type of lamps are quite non-linear. Lamp ignition occurs during each half cycle when the applied ac voltage reaches some required firing potential. There are also substantial increase in harmonics on the distribution system due to increased use of variable speed motors, dimmer switches, microwave ovens, television sets, battery changers etc for the future there may be many power driven coming n lines as harmonic sources such as fuel cells, battery storage devices, photovoltaic cells, battery storage devices, photovoltaic cells, wind generator and MHD. These devices will also have an impact on the power system. The equipment not only generates harmonics but in cases where shunt filters are used also amplifies the system harmonics by causing resonance with the ac network impedance. As many other forms of pollution the generation of harmonics effects the whole (electrical) environment and probably at much longer distances from the point of origin.

Perhaps the most obvious consequences of power system harmonics in the degradation of telephone communication caused by induced harmonic noise. However, therefore other less audible, though often more disastrous effects such as the maloperation of important control and protective equipment and the overloading of power apparatus and systems. Very often the existence of waveform pollution is only detected following excessive casualties (like the destruction of power factor correction capacitors) moreover, in the absence of an electrical welfare state, the casualties have to be repaired or replaced and the equivalent protected by filters at the customers expense, even through such preventive measures provide a general environment improvement.

The effect of these harmonics on cables, generators, transformers and other loads represents very important serious problem. To determine the impact of these harmonic flows on the distribution and transmission network and to eliminate the harmonics by suitable design of harmonic filters. The magnitude and phase of harmonic currents flowing in all the elements of the power network must be calculated.

1.2 STATE-OF-ART

Harmonic analysis is the process of calculating the magnitudes and phases of the fundamental and higher order harmonics of the periodic waveform. The resulting series is known as fourier series and establishes a relationship between a time domain

LIST OF TABLES

Table No	Caption	Page No
4.1	Result of test 1	34
4.2	Result of test 2	34

and that function in the frequency domain. J.B.J. Fourier (1768-1830) set up the basis for harmonic calculations.

With reference to power system harmonics, Steinmetz is one of the best known engineer who studied the power system harmonics and who published the result in the Transaction of the American Institute of Electrical Engineers(AIEE) (1900-1910). In general, the early studies were often relegated to harmonics produced by transformers non-linearity and results usually centered on the applicability of wye-delta connections.

But the electrification of railroads in California in 1914 produced interests in rectifier loads and telephone influence and the interference in the 600-Hertz range. The methods used by early investigators for the reduction of harmonic interference has greatly influenced the later work. Later filtering was added. Modern literature on power system harmonic problem analysis and solution is mostly of the case history type [1] when the harmonic signal strength is low. The assumption of sinusoidal analysis considerably.

1.2.1 Mathematical Models for Harmonic Power Flow

Some of the available literature on the mathematical models are the following :

Pilleggi et al. [2] presented a workable mathematical model for specific devices which are known to inject harmonics into power distribution system namely ac/dc converter. An equivalent PI transmission line model has presented in [3]. Arrillaga et al. [4] have explored the modeling of ac system and converter plant components needed to assess the level of zero sequence harmonic generation in the transmission line connected to larger converter plants. Arrillaga et al. [5] have presented the three phase modelling of an a.c. transmission system for harmonic penetration studies. Circuit coupling and impedance are incorporated in a simulation process. Arrillaga et al. [6] presented a mathematical model in the form of a Norton equivalent to represent the harmonic behavior of the transformer magnetizing branch. The model is, equally applicable in the presence of sinusoidal, non-sinusoidal and asymmetrical over excitation. Any number of harmonics can be modelled simultaneously. In reference [7] a generalised steady state model of the synchronous machine was presented, which can be taken into account any asymmetry or distortion presented in the armature voltages. They have showed that the field voltage is perfect d.c. The harmonic model of the

machine becomes a +ve admittance matrix. Carpinelli et al. [8] developed a generalised model of line commutated converters for the iterative harmonic analysis to avoid convergence problems and to save the accuracy of the results as well as computational efficiency.

1.2.2 Harmonic Power Flow Methods

Some of the methods available in literature are the following:

Xia and Heydt [9] have presented the modified Newton-Raphson power flow algorithm to accommodate non-linear loads without the assumption of superposition, radial circuitary or sinusoidal bus voltages. Grady et al. [10] developed a method to determine low audio range power system harmonics created by the non-linear loads and line commutated converters and incorporated into a harmonic power flow program. This method employs a Newton-Raphson solution technique that can model non-linear loads in inter-connected as well as in radial system. In reference [11] Tamby et al., described the salient features of harmonic flow program Q`HARM.

Heydt [12] presented a reverse power flow procedure to identify the source of harmonic signals in electric power system. In this procedure, the line and bus data at several points in the network are used with a least square estimator to calculate the injection spectrum at buses suspect of being harmonic source.

Xu and Matri et al. [13] developed a multiphase harmonic load flow (MHLF) technique for the harmonic analysis of static compensators and other non-linear devices under balanced or unbalanced conditions. The harmonic load flow is obtained from the interaction between the Norton equivalent circuit of the non-linear elements and the linear network at harmonic frequencies, in the reference [14] Girggis et al. presented an optimal measurement scheme for tracking the harmonics in power system voltage and current. They have introduced the new concept based on Kalman filtering theory for the optimal estimation of the parameters of time varying harmonics.

Vinay Sharma et al in [15] presented a method based upon the frequency domain analysis, which is utilised in conjunction with the fundamental load flow calculations for computing a harmonic voltage profile on a power system. Valcarcel et al. [16] presented a two step harmonic power flow algorithm that analyses harmonics in unbalanced systems. The first step is the fundamental frequency power flow for the ac

linear network in which non-linear loads are represented by current sources. The second is a frequency domain iterative Newton-Raphson method.

In reference [17] Carbone et al. presented a improved technique called as "preliminary step technique" which is a combination of time-domain simulation and iterative harmonic analysis. They have also presented another method called "Reactance pair technique" to improve the convergence properties. Caramia et al. [18] developed a probabilistic method for assessing harmonic distortion level in a power system. This method is extremely useful for analysing multiconverter system. Proposed method utilises a Monte Carlo simulation technique.

In reference [19] Arrillaga et al. described the structure of the harmonic domain, a new frame of reference for the harmonic analysis of power systems. It utilises the Newton-Raphson technique.

1.2.3 Artificial Neural Networks

With the development of artificial intelligence and neural network in recent years, there is a growing interest in applying these approaches to power system problems. A few papers are found in the literature in the field of power system harmonic analysis.

In reference [22], Widrow et al. described the history, origination operating characteristics and basic theory of several supervised neural network training algorithms including the perceptron rule, the LMD algorithm and the back-propagation technique. Hartana et al. [23] used a neural network approach to make initial estimates of harmonic sources in a power system with non-linear loads and relatively few permanent harmonic instruments.

Mori et al. [24] presented a neural network based method for predicting voltage harmonics in power system. The three-layered neural network was constructed with the back-propagation algorithm. The characteristic of input and hidden units are examined and concluded that the number of input units has more influence on the model accuracy than the number of hidden units in constructing the network.

Dash et al. [25] presented a new approach for the estimation of harmonic components of a power system using a linear adaptive neurons called Adeline.

Adaptive tracking of components of power system can easily be done using this technique.

1.3 OBJECTIVES OF PRESENT STUDY

The present study is an effort to use a neural network based approach to estimate a harmonic sources in a power system. Although many conventional methods available in the literature, they are less accurate during randomly varying load conditions. The present study aims to develop a three layered feed forward neural network with back-propagation learning scheme and train the neural net with a 18 bus system example and test to estimate unknown harmonic sources.

1.4 ORGANISATION OF DISSERTATION

Chapter II presents the mathematical modelling of various power system components and Newton-Raphson technique as well as sparsity programming technique, which are used for the harmonic power flow analysis of a system.

Chapter III introduces the artificial neural networks, describes the architecture of ANN, error minimization and weight change computation, based on back-propagation error learning algorithm.

Chapter IV presents the neural network training process for estimating harmonic sources and gives the results.

Chapter 2

Harmonic Power Flow Analysis

The non-linearity of a load results in a non-sinusoidal load current which is periodic and possesses a Fourier expansion, the non-sinusoidal load current passing through the network results in non-sinusoidal periodic voltages which also possess Fourier expansions. The higher frequency terms in these expressions are termed harmonics.

2.1 DEFINITIONS RELATED TO HARMONICS

Harmonic analysis requires definitions and mathematical relationships beyond those of ordinary fundamental frequency network analysis. Their definitions of active power, reactive voltamperes, distortion voltamperes and apparent voltamperes are based on Fourier series expansions for voltage and current. It has been shown in Grady [10] that in a balanced bilateral system, the even order harmonics and the d.c. offsets do not exist. Under these assumptions, the following definitions apply to the harmonic power flow algorithm.

Voltage

$$V(t) = \sum_{k=1}^h a_k \sin(k\omega_0 t + \delta_k), \quad k \text{ odd} \quad (2.1)$$

Current

$$i(t) = \sum_{k=1}^h c_k \sin(k\omega_0 t + \phi_k), \quad k \text{ odd} \quad (2.2)$$

Active Power

$$P = \sum_{k=1}^h a_k c_k \cos(\delta_k - \phi_k), \quad k \text{ odd} \quad (2.3)$$

Reactive Voltamperes

$$Q = \sum_{k=1}^h a_k c_k \sin(\delta_k - \phi_k), \quad k \text{ odd} \quad (2.4)$$

Root Mean Square Voltage and Current

$$V_{RMS} = \left[\sum_{k=1}^h a_k^2 \right]^{1/2}, \quad I_{RMS} = \left[\sum_{k=1}^h c_k^2 \right]^{1/2}, \quad k \text{ odd} \quad (2.5)$$

Apparent Voltamperes and Distortion Voltamperes

$$S = V_{RMS} I_{RMS}, \quad D = \sqrt{S^2 - P^2 - Q^2} \quad (2.6)$$

Power Factor

$$PF = \frac{P}{S} \quad (2.7)$$

Harmonic Distortion of Voltage and Current

$$HD_V = \frac{\left[\sum_{k=3}^h a_k^2 \right]^{1/2}}{V_{RMS}}, \quad HD_I = \frac{\left[\sum_{k=3}^h c_k^2 \right]^{1/2}}{I_{RMS}}, \quad k \text{ odd} \quad (2.8)$$

To analyse the harmonic propagation in an ac network, proper modelling of the various components in the network in the harmonic domain is necessary. In the next section, modelling of various components in the network is discussed in detail.

2.2 MODELLING OF NETWORK COMPONENTS

The modelling emphasis is restricted to harmonic orders in the low audio range (fundamental to the 25-50th multiple). Interaction between voltage and current harmonics of different order in a non-linear device is permitted, i.e., non-linearities are assumed to be equally distributed among the three phases.

2.2.1 Transmission Line Model

In the harmonic power flow algorithm, it is assumed that the transmission network is linear with no interaction between harmonics of different frequencies. Under perfectly balanced conditions, three phase transmission lines can be represented by their single-phase positive sequence models and nominal PI circuits. For a long line a number of PI models are connected in series to improve the accuracy of voltages and currents, which are affected by standing wave effects. As the frequency increase, the number of nominal PI sections to maintain a particularly accuracy increases

proportionally. On the other hand, the computational effort can be greatly reduced and simultaneously, the accuracy can be improved with the use of an equivalent PI model derived from the solution of the second order linear differential equations describing wave propagation phenomenon along the transmission lines.

The equivalent PI model in Fig. 2.1 is obtained from the nominal PI model by applying correction factors to the series impedance and shunt admittance's as given in [10,25].

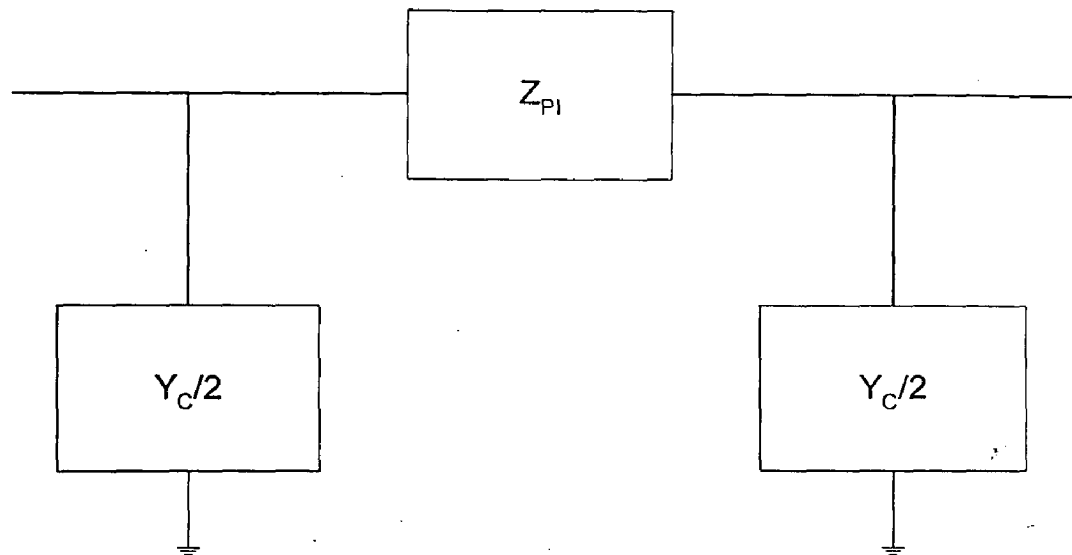


Figure 2.1 : Equivalent PI Representation of long transmission line

$$G_L + jB_L = Z_{PI} = Z \left(\frac{\sinh \gamma l}{\gamma l} \right) \quad (2.9)$$

$$Y_c / 2 = \frac{\gamma l}{2} \tanh \frac{\gamma l}{2} \quad (2.10)$$

where, $\gamma = \sqrt{zy}$

$$Z = zl$$

l = length of transmission line in miles

z = series impedance of line/mile

y = shunt admittance of line/mile

As frequency increases, the skin effect begins to dominate the resistance of the line. The approximate formula for evaluating the skin effect [10] is given by,

$$x = \frac{r_{ac}}{r_{dc}} = 0.175 \sqrt{\frac{k}{r_{dc}}} + 0.288 \quad (2.11)$$

where k is the harmonic number and r_{ac} , r_{dc} are the ac and dc resistance per unit length of the conductor (ohms per mile) respectively.

In the bundled conductor case, r_{dc} is the per phase conductor value. Using this formula for evaluating the skin effect, the per conductor ac resistance in the k^{th} harmonic order is obtained.

2.2.2 Synchronous Machines Model

When harmonic currents flow from the network into the stator windings of a generator, they create a flux rotating at a speed greater than the speed of the rotor. Thus the harmonics react with both the direct and quadrature axis inductances. effective average inductance[4,10] experienced by the positive or negative sequence odd harmonic current is given by

$$L_k = k \left[\frac{L_d'' + L_q''}{2} \right] \quad k > 1 \quad (2.12)$$

where k is the harmonic order and L_d'' , L_q'' are the direct and quadrature axis subtransient inductances. Based on equation. (2.12), the basic model of a synchronous generator for harmonic power flow study is given in fig Fig. 2.2. P_g , Q_g and $V^{(1)}$ are fundamental frequency active Reactive power generation and voltage respectively.

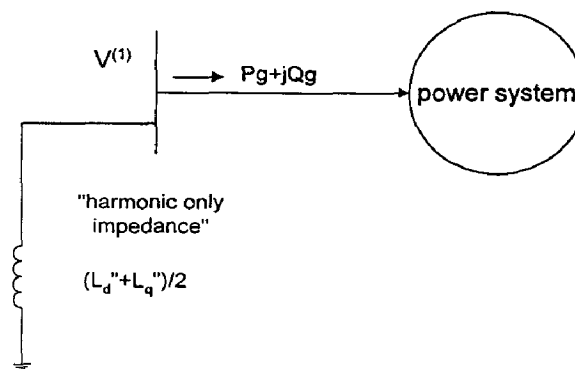


Figure 2.2 : Power Flow Model of Synchronous Model

2.2.3 Load Models

It is difficult to model accurately most system load buses since the exact composition of loads at that bus is usually unknown. Certainly, induction motors and heating and lighting loads are major components of a system bus load. Pileggi et al. [3] suggested that in the absence of the information regarding specific load composition at a bus, the load should be modelled as a shunt resistor in parallel with a suitable inductor or capacitor to account for the active and reactive power at 60 Hz respectively. This is referred to as a "generalized conventional load" model as shown in Fig. 2.3.

$$\text{Resistance} \quad : \quad R = [V^{(1)}]^2 / P_L$$

$$\text{Inductance} \quad : \quad L = [V^{(1)}]^2 / Q_L$$

Where $V^{(1)}$, P_L and Q_L are fundamental frequency voltage, active and reactive loads respectively.

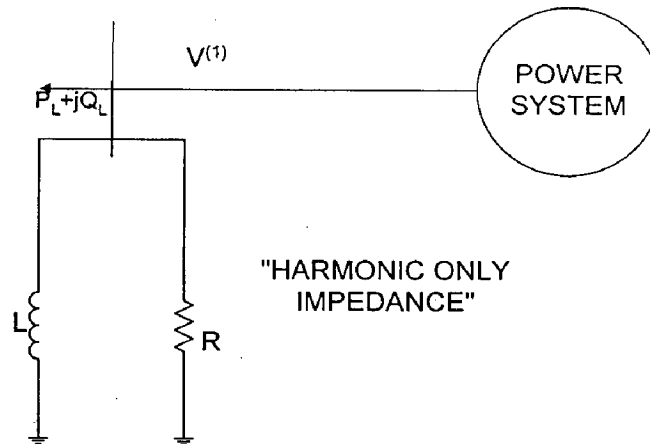


Figure 2.3 : Power Flow Model Of a Generalized Conventional Load

2.2.4 Modelling of Other Network Elements

Other network elements such as reactors, capacitors and transformers are modelled [5,9] as lumped impedances, which vary with frequency according to the usual sinusoidal steady state impedance formulas. The connection configuration of these elements (i.e., wye-wye, grounded wye-delta etc.) is used to modify the zero sequence impedance appropriately. Three phase transformer connections are represented by complex turns ratios which account for the -30° , 0° or $+30^\circ$ phase shift at various harmonic frequencies.

2.2.5 Non-linear Resistive Load Model

Due to their widespread use and being significant sources of harmonics, the gaseous discharge lamps (fluorescent, mercury arc and sodium discharge types) are included in this study. Grady and Heydt [10] developed a relationship between instantaneous currents and voltage for the lamp as given by,

$$\begin{aligned} i(t) &= B \sum_{k=1}^N b_k V^k(t), \quad k \text{ odd, } N \text{ odd} \\ &= \sum_{k=1}^h c^{(k)} \sin(k\omega_o t + \gamma^{(k)}), \quad k \text{ odd, } h \text{ odd} \end{aligned} \quad (2.13)$$

The coefficients b_1, b_3, b_5 are calculated by comparison with actual measured results with sinusoidal applied voltage. This model assumes only odd powers of and odd harmonics in the applied voltage. The "b" coefficients are kept constant at the predetermined values. while B, the non-linear resistor state variable is dependent on the real power drawn by the resistor and the terminal voltage. What is required is an expression for the current drawn by the non-linear resistor in the following form,

$$i(t) = \sum_{k=1}^h c^{(k)} \sin(k\omega_o t + \phi^{(k)}) \quad (2.14)$$

where h is the highest harmonic of interest in order to transform the eq. (2.13) to the form of eq. (2.14). The values of $V(t)$ for the full range of one fundamental cycle as a function of time are first considered. Fourier series for voltage is

$$V(t) = \sum_{k=1}^h V^{(k)} \sin(k\omega_o t + \delta^{(k)}), \quad k \text{ odd, } h \text{ odd} \quad (2.15)$$

The instantaneous values of $i_1(t)$ are calculated for these samples of $V(t)$ using

$$i_1(t) = b_1 V(t) + b_3 V^3(t) + b_5 V^5(t) + \dots \quad (2.16)$$

Having thus obtained the instantaneous values of $i_1(t)$ for one fundamental cycle an FFT program is used to get eq. (2.16) in the form of eq. (2.15)

$$i_1(t) = \sum_{k=1}^n A_k \sin(k\omega t + \gamma_k), \quad k \text{ odd} \quad (2.17)$$

Since $i(t) = Bi_1(t)$ we have reduced our problem to one of determining B. The real power consumed by the non-linear resistor can be expressed in terms of the harmonic voltages and currents as,

$$P = \sum_{k=1}^n \frac{V_{km} I_{km}}{2} \cos(\theta_k - \gamma_k) \quad k \text{ odd} \quad (2.18)$$

It can also be expressed as

$$P = B \left[\sum_{k=1}^n \frac{V_{km} A_k}{2} \cos(\theta_k - \gamma_k) \right] \quad k \text{ odd} \quad (2.19)$$

From equations (2.18) and (2.19), the value of B can be calculated.

The necessary partial derivation for the harmonic Jacobian matrix may be determined by examining

$$i(t) = \sum_{k=1}^n \left[c^{(k)} \left[\cos(kw_o t) \cos(\phi^{(k)}) - \sin(kw_o t) \sin(\phi_1^{(k)}) \right] \right] \quad (2.20)$$

$$i(t) = \sum_{k=1}^n \left[I_i^{(k)} \cos(kw_o t) + I_r^{(k)} \sin(kw_o t) \right] \quad (2.21)$$

where $I^{(k)}$ is the magnitude of the kth harmonic phasor component of $i(t)$ and $I_r^{(k)}$ and $I_i^{(k)}$ signify the real and imaginary components. The partial derivative of $I_r^{(k)}$ and $I_i^{(k)}$ with respect to harmonic voltage magnitude and phase angles and with respect to variable B are readily obtained. For use in a harmonic power flow study, these partial derivatives are substituted into the Jacobian matrices.

2.2.6 Modeling of Converter

The generation of harmonic currents at a rectifier load is a complex phenomenon if the bus voltage is non-sinusoidal. Reference [9,10] gives an iterative procedure for the analysis of both six and twelve pulse bridges. For a six pulse bridge, the six regions of $i(t)$ (load currents) are calculated by the solution of the appropriate differential equation which can be obtained by applying Kirchoff's voltage law for the R-L circuit. Fig. 2.4 shows a three-phase full wave bridge rectifier with a general load consisting of passive elements resistance R and filter inductance F and d.c. voltage. The three-phase transformer is pictorially shown in this figure and may be connected in a variety of three phase connections. The turns ratio $1:\exp(j\beta_s)$ is determined by the connections of windings and the sequence of applied voltage. For the full wave rectifier, only k-th harmonic orders, where $k = 1, 5, 7, \dots$ occur in the system. For other non-linear loads,

harmonics of specified values of k may or may not exist depending on transformer connection and type of non-linearity.

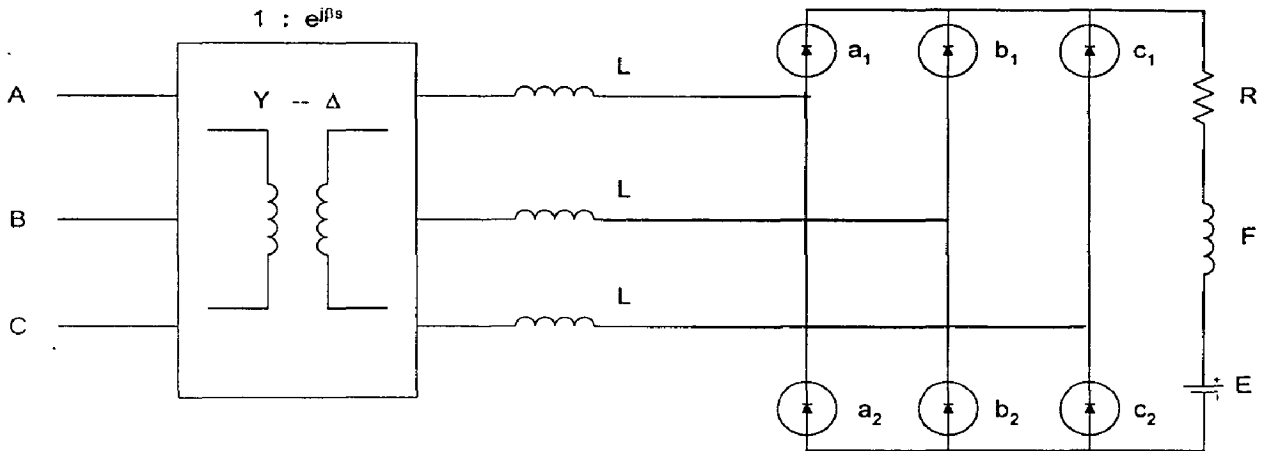


Figure 2.4 : Full Wave Six Pulse Bridge Rectifier

The resulting load phase currents can be expressed in a fourier series with odd terms only.

$$I_a(t) = \sum_l (I_l^{(i)} \cos(l\omega t) + I_l^{(r)} \sin(l\omega t)); \quad l = 1, 5, 7, 11, 13 \quad (2.22)$$

$$I_l^{(i)} = \frac{2}{\pi} \int_{\alpha}^{\pi+\alpha} i_a(t) \cos(l\omega t) d(\omega t) \quad (2.23)$$

$$I_l^{(r)} = \frac{2}{\pi} \int_{\alpha}^{\pi+\alpha} i_a(t) \sin(l\omega t) d(\omega t) \quad (2.24)$$

Equation (2.22) to (2.24) are valid for any α (the firing angle). Then the integration period in (2.23&2.24) is divided into six periods in each of which $i_a(t)$ is known. The six regions are denoted by superscript $i=1,2,\dots,6$ on i_a and the general expression for region i is given by [4],

$$i_a^{(i)} = A^{(i)} + B^{(i)} e^{p^{(i)}t} + \sum_k Y_k^{(i)} u_k \sin(k\omega t + \phi_k^{(i)} + \theta)$$

After substituting the values of A, B, Y, θ and p in the above equation, (the values of all these constants are explained in Appendix B), we get fourier expansion of load current.

$$\begin{aligned}
I_i^{(l)} &= \frac{2}{\pi} \sum_{m=1}^6 \left[\int_{\gamma_1^{(m)}}^{\gamma_2^{(m)}} (A^{(m)} + B^{(m)} e^{p^{(m)}t}) \cos(l\omega t) d(\omega t) \right. \\
&\quad \left. + \sum_k Y_k^{(m)} u_k \int_{\gamma_1^{(m)}}^{\gamma_2^{(m)}} \sin(k\omega t + \phi_k + \theta_k^{(m)}) \cos(l\omega t) d(\omega t) \right] \\
&= I_{i,T}^{(l)} + I_{i,S}^{(l)} \tag{2.25}
\end{aligned}$$

$$\begin{aligned}
I_r^{(l)} &= \frac{2}{\pi} \sum_{m=1}^6 \left[\int_{\gamma_1^{(m)}}^{\gamma_2^{(m)}} (A^{(m)} + B^{(m)} e^{p^{(m)}t}) \sin(l\omega t) d(\omega t) \right. \\
&\quad \left. + \sum_k Y_k^{(m)} u_k \int_{\gamma_1^{(m)}}^{\gamma_2^{(m)}} \sin(k\omega t + \phi_k + \theta_k^{(m)}) \sin(l\omega t) d(\omega t) \right] \\
&= I_{r,T}^{(l)} + I_{r,S}^{(l)} \tag{2.26}
\end{aligned}$$

$$I_{i,T}^{(l)} = \frac{2}{\pi} \sum_m \left[A^{(m)} \frac{\sin l\omega t}{l} \Big|_{\gamma_1^{(m)}}^{\gamma_2^{(m)}} + B^{(m)} \frac{e^{p^{(m)}t} (p^{(m)} \cos l\omega t + l \sin l\omega t)}{(p^{(m)})^2 + l^2} \Big|_{\gamma_1^{(m)}}^{\gamma_2^{(m)}} \right]$$

$$I_{r,T}^{(l)} = \frac{2}{\pi} \sum_m \left[-A^{(m)} \frac{\cos l\omega t}{l} \Big|_{\gamma_1^{(m)}}^{\gamma_2^{(m)}} + B^{(m)} \frac{e^{p^{(m)}t} (p^{(m)} \sin l\omega t + l \cos l\omega t)}{(p^{(m)})^2 + l^2} \Big|_{\gamma_1^{(m)}}^{\gamma_2^{(m)}} \right]$$

$$\begin{aligned}
I_{i,S}^{(l)} &= \frac{2}{\pi} \sum_m \left[\sum_k \frac{Y_k^{(m)} u_k}{2} \left[\frac{\cos((k+l)\omega t + \phi_k + \theta_k^{(m)})}{-k-l} \right] \right. \\
&\quad \left. + \sum_k \frac{Y_k^{(m)} u_k}{2} \left[\frac{\cos((k-l)\omega t + \phi_k + \theta_k^{(m)})}{-k+l} \right] \right. \\
&\quad \left. + \frac{Y_l^{(m)} u_l}{2} t \sin(\phi_l + \phi_l^{(m)}) \right]
\end{aligned}$$

$$\begin{aligned}
I_{r,S}^{(l)} &= \frac{2}{\pi} \sum_m \left[\sum_k \frac{Y_k^{(m)} u_k}{2} \left[\frac{\sin((k+l)\omega t + \phi_k + \theta_k^{(m)})}{-k-l} \right] \right. \\
&\quad \left. + \sum_k \frac{Y_k^{(m)} u_k}{2} \left[\frac{\sin((k-l)\omega t + \phi_k + \theta_k^{(m)})}{-k+l} \right] \right. \\
&\quad \left. + \frac{Y_l^{(m)} u_l}{2} t \cos(\phi_l + \phi_l^{(m)}) \right] \tag{2.27}
\end{aligned}$$

Partial derivatives of $I_{i,T}^{(l)}$ through $I_{r,s}^{(l)}$ will be used in a Newton-Raphson as a element of Jacobian matrix.

The d.c. current I_d is given by [20],

$$I_d = \frac{\sqrt{2}}{2\pi} \sum_k \frac{V^{(k)}\delta_k}{k} \left[\cos(\theta^{(k)} - k\theta^{(1)} + k\alpha) - \cos(\theta^{(k)} - k\theta^{(1)} + k\delta) \right] \quad (2.28)$$

where $V^{(k)}$ is the line to line ac kth harmonic voltages and

x_c is the equivalent fundamental reactance in the converter circuit

δ^k is the triplet.

$$\delta_k = \begin{cases} 1 & \text{if } k \text{ in positive sequence} \\ -1 & \text{if } k \text{ in negative sequence} \\ 0 & \text{if } k \text{ in zero sequence} \end{cases}$$

Similarly DC voltage is given by,

$$V_d = \frac{3\sqrt{2}}{2\pi} \sum_k \frac{V^{(k)}\delta_k}{k} \left[\cos(\theta^{(k)} - k\theta^{(1)} + k\alpha) - \cos(\theta^{(k)} - k\theta^{(1)} + k\delta) \right] \quad (2.29)$$

Power transmitted through the converter is,

$$P_d = V_d I_d = C \sum_{k,l} \frac{V^{(k)}V^{(l)}\delta_k\delta_l}{kl} \left[\cos(\theta^{(k)} - k\theta^{(1)} + k\alpha) \cos(\theta^{(l)} - l\theta^{(1)} + l\alpha) - \cos(\theta^{(k)} - k\theta^{(1)} + k\delta) \cos(\theta^{(l)} - l\theta^{(1)} + l\delta) \right] \quad (2.30)$$

Where, $C = 3/(2\pi x_c)$.

Based on the above modelling techniques, the Newton-Raphson method for solving harmonic power flow problem is described in the next section.

2.3 NEWTON-RAPHSON METHOD FOR HARMONIC LOAD FLOW ANALYSIS

Newton-Raphson method for power flow study solution is well known. The mismatch equations, i.e., active power and reactive power balances are forced to zero iteratively by forcing the bus voltages towards the solution.

Consider bus 1 to be slack bus, buses 2 through m-1 are conventional load buses (linear loads : P-V or P-Q buses) and buses m through n as non-sinusoidal load buses. Buses 1 through m-1 are handled in the usual way. For buses m through n inclusive, the

active power P is specified and apparent voltampères are known. Also the form of the non-linearity is known. The power balance equations are that ΔP and ΔQ at all non-slack buses is zero for all harmonics. The functional forms of ΔP and ΔQ as a function of $|V_{bus}|$ and Q_{bus} (i.e., bus voltage magnitudes and phase angles) is as in the conventional case with that Y_{bus} must be modified at harmonic frequencies. The specified values of P^s and Q^s are known at buses 2 through $m-1$. But only $P^{(1)}$ is known at buses m through n . The above formulation is insufficient to solve the harmonic power flow problem. Two additional relations are required: current balance and apparent volt-ampere balance. The current balance is written for the fundamental frequency ($s = 1$) as (only converter loads are considered, incase of Non-Linear Resistive loads the expressions for currents have been explained in section 2.2.5)

$$\begin{bmatrix} I_{r,m}^{(1)} \\ I_{i,m}^{(1)} \\ I_{r,m+1}^{(1)} \\ I_{i,m+1}^{(1)} \\ \dots \\ I_{i,n}^{(1)} \end{bmatrix} = \begin{bmatrix} g_{r,m}^{(1)}(v_m^{(1)}, v_m^{(5)}, \dots, \alpha_m, \beta_m) \\ g_{i,m}^{(1)}(v_m^{(1)}, v_m^{(5)}, \dots, \alpha_m, \beta_m) \\ \dots \\ g_{i,n}^{(1)}(v_n^{(1)}, v_n^{(5)}, \dots, \alpha_n, \beta_n) \end{bmatrix} \quad (2.31)$$

where $I_{r,m}^{(1)}$ and $I_{i,m}^{(1)}$ are the real and imaginary bus injection currents at bus m , harmonic 1. α_m is the triggering angle at bus m , and β_m is commuting resistance or d.c. voltage, expressions for the I terms in (2.31) are given in eq. (2.27). Also eq. (2.31) is rewritten for $s \neq 1$ (i.e., for harmonics)

$$\begin{bmatrix} I_{r,1}^{(1)} \\ I_{i,1}^{(1)} \\ \dots \\ I_{r,m-1}^{(1)} \\ I_{r,m}^{(1)} \\ I_{i,m}^{(1)} \\ \dots \\ I_{i,n}^{(1)} \end{bmatrix} = \begin{bmatrix} 0 \\ \dots \\ g_{r,m}^{(k)}(v_m^{(1)}, v_m^{(5)}, \dots, \alpha_m, \beta_m) \\ g_{i,m}^{(k)}(v_m^{(1)}, v_m^{(5)}, \dots, \alpha_m, \beta_m) \\ \dots \\ g_{i,n}^{(k)}(v_n^{(1)}, v_n^{(5)}, \dots, \alpha_n, \beta_n) \end{bmatrix} \quad (2.32)$$

Again, the current expressions are given in eq. (2.27).

The apparent volt-ampere balance at each bus

$$S_l^2 = \sum_s (P_l^{(s)})^2 + \sum_s (Q_l^{(s)})^2 + \sum D_l^2 \quad (2.33)$$

where $l = m, \dots, n$ and $\sum D_l^2$ denotes the total distortion voltages at bus .

Since D_m, \dots, D_l can be calculated from $g_{r,m}, g_{i,m}, \dots, g_{i,n}$. these distortion voltamperes are not treated as independent variables.

Total number of equations required for the harmonic power flow is $2(1+h)n + 3N$.

These are power balance equations	:	$2(n-1)$.
Swing bus voltage and swing bus angle	:	2
current balance equations (2.31) & (2.32)	:	$2nh$
apparent volt-ampere balance equation (2.29)	:	N .

The number of unknowns is accounted as follows :

Bus voltage magnitudes and angles for all harmonics plus fundamentals	:	$2n(1+h)$
Total reactive voltamp at each non-linear load bus	:	N
α and β at each rectifier bus	:	$2N$

Hence there are $2(1+h)n + 3N$ unknowns.

Newton's method is formulated by forcing the appropriate mismatches. ΔM to zero using a Jacobian matrix, J , and obtaining appropriate correction term ΔU .

$$\Delta M = J \Delta U$$

$$\begin{bmatrix} \Delta W \\ \Delta I^{(1)} \\ \Delta I^{(5)} \\ \Delta I^{(7)} \\ \dots \end{bmatrix} = \begin{bmatrix} J^{(1)} & J^{(5)} & J^{(7)} & \dots & 0 \\ YG^{(1,1)} & YG^{(1,5)} & YG^{(1,7)} & \dots & H^{(1)} \\ YG^{(5,1)} & YG^{(5,5)} & YG^{(5,7)} & \dots & H^{(5)} \\ YG^{(7,1)} & YG^{(7,5)} & YG^{(7,7)} & \dots & H^{(7)} \end{bmatrix} \begin{bmatrix} \Delta V^{(1)} \\ \Delta V^{(5)} \\ \vdots \\ \Delta \alpha \end{bmatrix} \quad \text{----(2.34)}$$

where all elements in (2.34) are subvectors and submatrices partitioned from ΔM , J and ΔU . These sub-elements are,

$$\Delta V^{(k)} = (V_1^{(k)} \Delta \theta_1^{(k)}, \Delta V_1^{(k)}, \dots, \Delta V_n^{(k)})^t \quad k = 1, 5, 7$$

$$\Delta \alpha = (\Delta \alpha_m, \Delta \beta_m, \dots, \Delta \beta_n)^t$$

$$\Delta W = (P_1^{(s)} - f_{1,1}, Q_1^s - f_{1,2}, \dots, Q_n^s - f_{n,2})^t$$

= mismatch active power and reactive voltampere,

$$\Delta I^{(1)} = (I_{r,m}^{(1)} + g_{r,m}^{(1)}, I_{i,m}^{(1)} + g_{i,m}^{(1)}, \dots, I_{i,n}^{(1)} + g_{i,n}^{(1)})^t$$

= mismatch fundamental current

$$\Delta I^{(k)} = (I_{r,1}^{(k)}, I_{i,1}^{(k)}, \dots, I_{i,m-1}^{(k)}, I_{r,m}^{(k)} + g_{r,m}^{(k)}, I_{i,m}^{(k)} + g_{i,m}^{(k)}, \dots, I_{i,n}^{(k)} + g_{i,n}^{(k)})^t \quad k \neq 1$$

= mismatch harmonic currents

$$J^{(1)} = \text{conventional power flow study Jacobian}$$

$$j^{(k)} = \text{harmonic } k \text{ Jacobian}$$

$$= \left[\begin{array}{c} O_{2(m-1), 2n} \\ \hline \text{partial derivatives of } P \text{ and } Q \text{ w.r.t } V^{(k)} \text{ and } \theta^{(k)} \\ \text{These are formed in the conventional way} \end{array} \right] \quad \leftarrow \text{submatrix}$$

(note : $O_{2(m-1), 2n}$ denotes a $2(m-1)$ by $2n$ array of zeroes. Also note that Y_{bus} matrix used to generate $J^{(k)}$ is $Y_{bus}^{(k)}$. Also

$$(YG)^{(k,j)} = \begin{cases} Y^{(k,k)} + G^{(k,k)} & k = j \\ G^{(k,j)} & k \neq j \end{cases}$$

where $Y^{(k,k)}$ is an array of partial derivatives of injection currents (kth harmonic only) with respect to kth harmonic voltages and $G^{(k,j)}$ are the partials of the kth harmonic load current with respect to the jth harmonic supply voltages.

$G^{(k,j)}$ is given by,

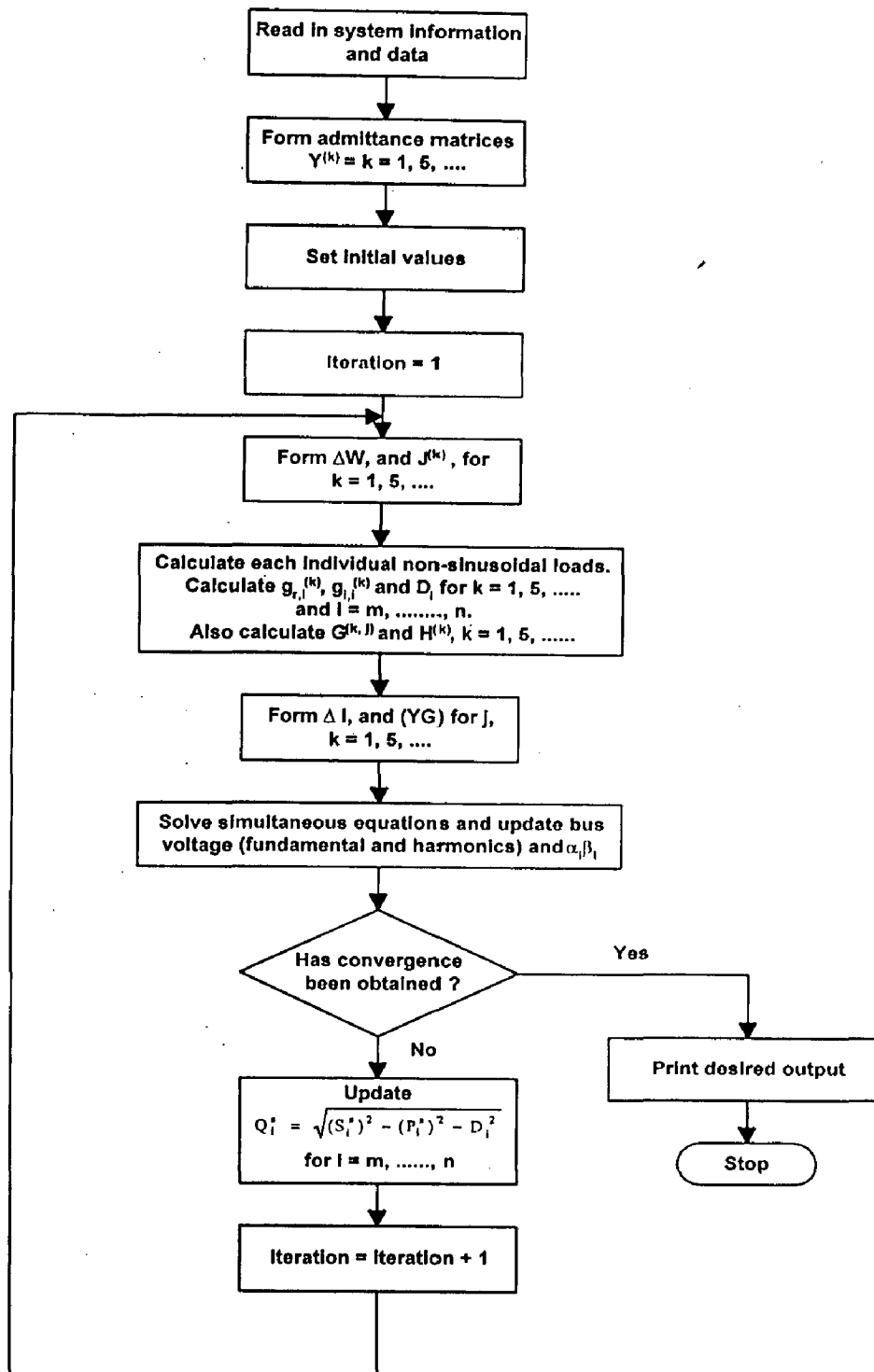
$O_{2(m-1),2(m-1)}$	$O_{2(m-1),2N}$		
	$\frac{\partial g_{rm}^{(k)}}{V_m^{(j)} \partial \theta_m^{(j)}} \quad \frac{\partial g_{rm}^{(k)}}{\partial V_m^{(j)}}$	0	0
	$\frac{\partial g_{im}^{(k)}}{V_m^{(j)} \partial \theta_m^{(j)}} \quad \frac{\partial g_{im}^{(k)}}{\partial V_m^{(j)}}$		
$O_{2N,2(m-)}$	0	...	0
	0		$\frac{\partial g_m^{(k)}}{V_n^{(j)} \partial \theta_n^{(j)}} \quad \frac{\partial g_m^{(k)}}{\partial V_n^{(j)}}$
	0	0	$\frac{\partial g_{im}^{(k)}}{V_n^{(j)} \partial \theta_n^{(j)}} \quad \frac{\partial g_{im}^{(k)}}{\partial V_n^{(j)}}$

Note that for $k = 1$, only the last $2N$ rows exist. These partials are found by differentiating the sinusoidal steady state parts of eq. (2.27) for harmonic loads. Also, $H^{(k)}$ is the partial derivative of non-sinusoidal loads real and imaginary currents with respect to triggering angle α and commutation resistance β .

$$H^{(k)} = \text{diag} \begin{bmatrix} \frac{\partial g_{rt}^{(k)}}{\partial \alpha t} & \frac{\partial g_{rt}^{(k)}}{\partial \beta t} \\ \frac{\partial g_{it}^{(k)}}{\partial \alpha t} & \frac{\partial g_{it}^{(k)}}{\partial \beta t} \end{bmatrix}$$

$$t = m, \dots, n; \quad k = 1, 5, 7, \dots$$

2.4. FLOW CHART FOR HARMONIC POWER FLOW



2.5 SPARSITY PROGRAMMING METHOD FOR THE HARMONIC POWER FLOW

The Jacobian matrix used in harmonic power flow studies is a sparse array of approximate dimensions twice the number of buses times the number of harmonics considered. The fundamental frequency vector is as sparse as Y_{bus} the remainder has

very large blocks of zeros which are wholly relegated to the upper right and lower left triangles. Also submatrices on the diagonal appear which are as sparse as Y_{bus} . For a 200 bus system in which 5 harmonics are considered, typically, the Jacobian is over 99% sparse unlike the fundamental Jacobian which relies on optimal ordering to obtain large blocks of zeros, in the harmonic case, large blocks of zeros occur independent of bus ordering. The diagonal entries are generally non-zero. It is approximate to examine a specially designed sparsity programming method suited for this case. One such method which has given excellent access time with reasonable storage requirements is termed the LLT-URT sparsity programming method with diagonal fixes. In this method, the diagonal entries are stored separately along with two parallel vectors which contain pointers. The first of these pointers point to a lower left triangle (LLT) array of non-zero matrices in the column corresponding to the diagonal position whence it was indexed. The second vector similarly contains pointers to the upper right triangle (URT) non-zero entries in the row corresponding to the diagonal position whence it was indexed. In parallel with the LLT non-zero entry vector is a vector containing the proper row number of that non-zero entry. Similarly, the URT array has a parallel vector containing column matrices.

Fig. 2.5 pictorially illustrates the method. The total storage (for an N_j square Jacobian and N_z non-zero entries half of which are in the URT half in the LLT) is $3N_j + 3N_z$. The access time to find an off diagonal entry is typically less than that required for 4 scans of a vector for the correct entry.

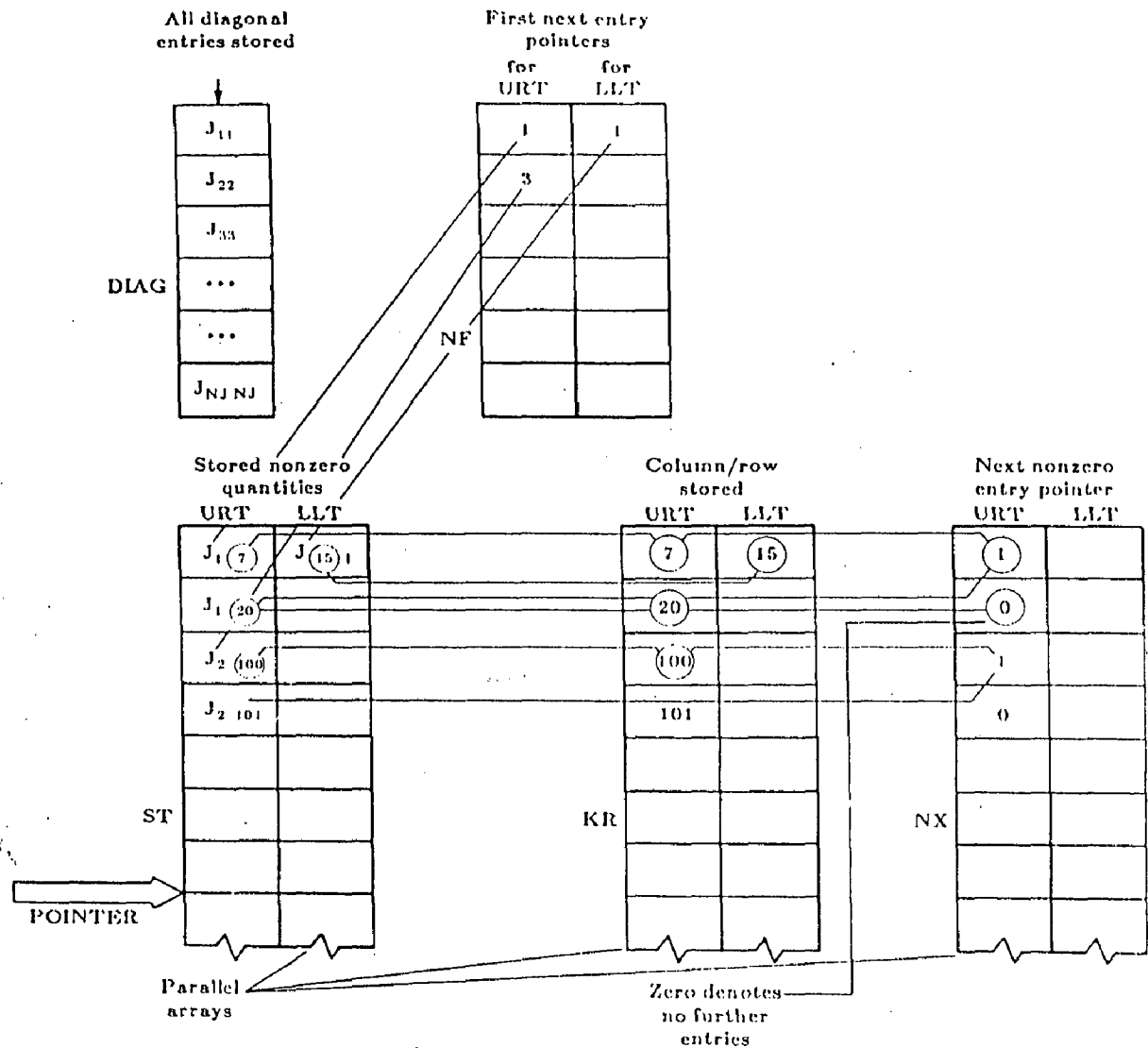


Figure 2.5 Sparsity storage technique using LLT/URT storage and chained data structures

Chapter 3

FEED FORWARD NEURAL NETWORKS

3.1 INTRODUCTION TO ANN

Neural network computing was developed as a method of using a large number of simple parallel processors to recognize preprogrammed or "learned" patterns. With the development of artificial neural network in recent years, there is growing interest in applying this approach to the area of power system. Neural systems gained popularity over other methods as they are efficient in discovering similarities among large bodies of data in distributed/fault tolerant models for non-linear, partly unknown, and noisy corrupted systems. Artificial neural network (ANN) is the functional imitation of a human brain which simulates the human intuition in making decisions and drawing conclusions even when presented with complex, noisy, irrelevant/partial information. The information going to the input layer units of ANN is recorded into an internal representation and the outputs are generated by the internal representation when excited by the input pattern. It can model any non-linear function without knowledge of the actual model structure and during testing phase it gives the result in very short time. A neural network consists of a number of neurons which are the elementary processing units that are connected together according to some pattern of connectivity.

A "connection" between a pair of neurons has an associated numerical strength called synaptic weight. The positive synaptic weight represents excitatory connection that increases the strength of connection, while negative weight represents inhibitory connection that decreases the strength of the connection between neurons. The development of ANN involves two phases, training phase and testing phase. Training of ANN is carried out by presenting the network with examples called training patterns. The synaptic weights get modified to represent the given problem accurately. Once the network has learnt the problem, it may be presented with new unknown patterns and its accuracy can be checked. This is called testing phase. Depending upon the training imparted, ANN can be classified as supervised ANN or unsupervised ANN.

The supervised ANN requires a set of inputs and outputs for its training. During the training period, the output obtained from the ANN is compared with the desired output (target) and the difference (rms error) is reduced by using some learning algorithm. The training is continued till the actual output reaches to an acceptable level. The trained ANN can then be used for testing purpose by providing unknown patterns to it. Supervised ANN may be feed forward or non-recurrent network such as Multi Layer Perception (MLP), Functional Link Net (FLN), and Radial Basin Function (RBF), or a feedback or recurrent ANN such as Hopfield network. To train a supervised ANN, various learning algorithms such as error back-propagation Widrow-Hoff learning rule, Hebbian learning rule etc. are established in the literature.

In unsupervised ANN, there are no expected outputs presented to neural network, as in a supervised training algorithm. Instead, a network, by its self-organizing properties, is able to infer relationships and learn as more inputs are presented to it.

In the present work, a supervised feedforward ANN with error back propagation training algorithm supervised has been used.

3.2 FEEDFORWARD BACKPROPAGATION NETWORK

The feedforward ANN with error training algorithm back propagation is a very popular model in neural network in literature. It does not have feed back connections, but errors are back propagated during training. In the following two subsections, the basic architecture and the training algorithm of the ANN is discussed briefly.

3.2.1 Architecture of the ANN

A typical three-layer feedforward backpropagation of network is shown in Fig. 3.1. The three layers are designated as input, hidden and output layers. In each layer, a number of actual processing elements or networks (nodes) are present. However, on the input layer, there are no processing elements. The nodes at the input layer simply function as the receiving points of the inputs. The nodes are connected from input to output layers via the hidden layer in a feedforward way.

§ 10, 178.

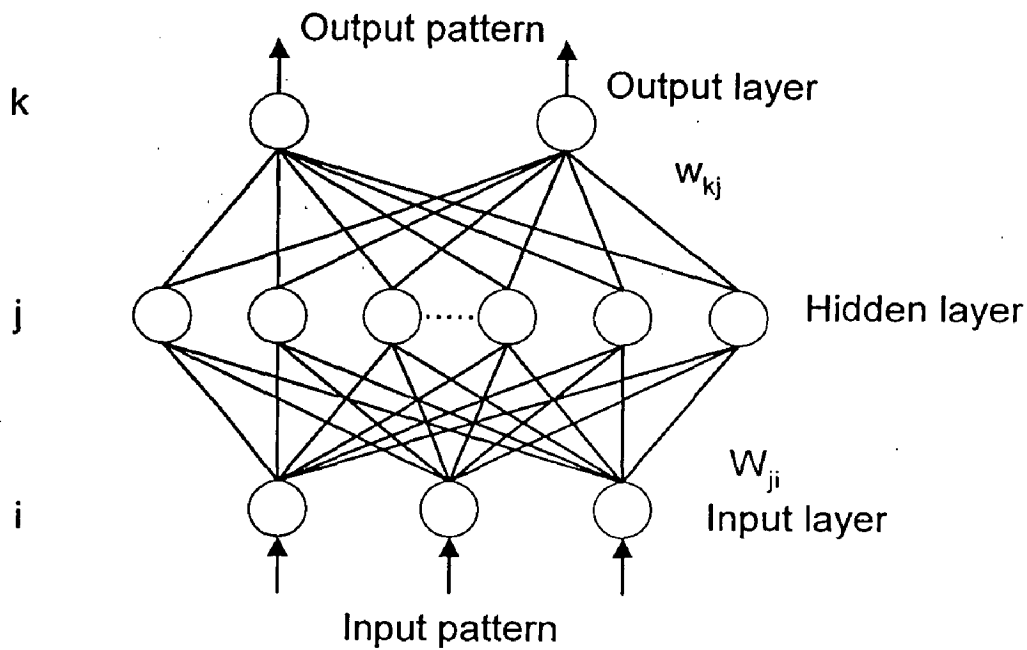


Figure 3.1 : Three-layer Feed Forward Neural Network

Now, consider relationship between input and output of a neuron. Defining output of unit i at the previous layer as O_i , the input of unit j at the present layer can be written as,

$$net_j = \sum_i W_{ij} O_i \quad (3.1)$$

where W_{ij} : weight between the units i of the previous layer and unit j of the present layer.

Fig. 3.2 depicts the relationship given by Eq. (3.1). Output O_j of unit j at the present layer is expressed by the following relation :

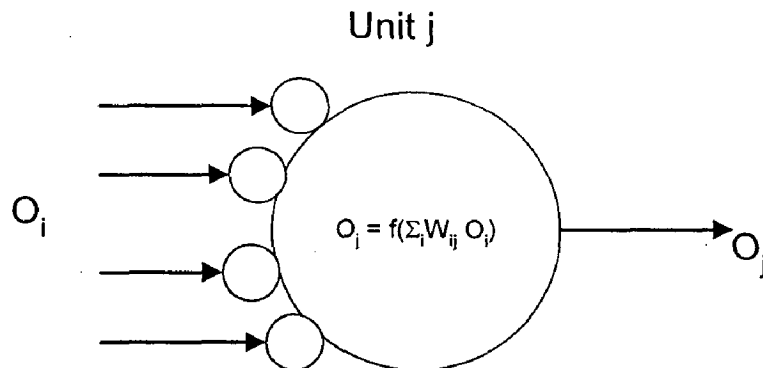


Figure 3.2 : A basic processing unit

$$O_j = f(\text{net}_j) \quad (3.2)$$

Where $f(x) = \text{sigmoid function}$ such as

$$f(x) = \frac{1}{1 + \exp(-x)} \quad (3.3)$$

$$\therefore O_j = \frac{1}{1 + e^{-\left(\sum_i w_{ij} O_i + \theta_j\right)}} \quad (3.4)$$

Where θ_j is the threshold or bias used to augment the input to any neuron.

The outputs of the hidden layer units are then transmitted to the inputs of the output layer through another weighted network in the same manner.

3.2.2 Error Minimization and Weight Change Computation

During training, the weights in the ANN are modified to minimize the total error E_r , which is the sum of squared difference between the set of training outputs for all patterns p , t_{pj} and the set of actual outputs O_{pj} .

$$E_r = \frac{1}{2} \sum_p \sum_j (t_{pj} - O_{pj})^2 \quad (3.5)$$

where t_{pj} : desired output at j th neuron at the output layer for pattern 'p' and

O_{pj} : the calculated value of the j th neuron at the output layer for pattern p .

The error E_r can be minimized by adjusting the weight between the units. The steepest descent method is utilised to modify the weights in order to minimize E_r .

The expressions for modifying the weights of the ANN are given by [30]:

$$w_{kj} = w_{kj} + \eta \delta_{ok} y_j \quad \text{for } k = 1, 2, \dots, K \text{ and } j = 1, 2, J \quad (3.6)$$

$$v_{ji} = v_{ji} + \eta \delta_{yj} z_i \quad \text{for } j = 1, 2, \dots, J \text{ and } i = 1, 2, I \quad (3.7)$$

$$\delta_{ok} = (d_k - O_k) (1 - O_k) O_k \quad \text{for } k = 1, 2, \dots, K \quad (3.8)$$

$$\delta_{yj} = y_j (1 - y_j) \sum_{k=1}^K \delta_{ok} w_{kj} \quad \text{for } j = 1, 2, \dots, J \quad (3.9)$$

where I : no. of input nodes

J : no. of hidden layer nodes

K : no. of output nodes

w_{kj} : weight between the k th node of the output layer and the j th node of the

hidden layer.

w_{ji} : interconnection weight between the j th node of the hidden layer and the i th node of the input layer.

d_k : desired output at the k th node of output layer

O_k : calculated output at the k th node of the output layer.

η : learning constant

z_i : input to the i th node of the input layer

y_j : input to the j th node of the hidden layer

δ_{ok} : error signal of the k th node of the output layer

δ_{yj} : error signal of the j th node in the hidden layer.

3.3 STEPWISE SOLUTION ALGORITHM

To obtain the input features of a neural network, which consists of 'fundamental voltages and load currents at the non-linear load buses and fundamental and complex harmonic line currents, a large number of load patterns are generated by perturbing the load at non-linear load buses and full harmonic load flow is carried out by using PCFLO program which was developed by W.M.Grady. Neural networks are trained till the error between the desired output and that obtained from the neural network is reduced significantly.

The solution algorithm for estimating the harmonics by using back-propagation algorithm can be summarized in the following steps.

Step 1 : Assign the input signals to unit at the input layer.

Step 2 : Set the maximum number of iterations IT^{\max} and Number of training patterns IP^{\max}

Step 3 : Initialise weights randomly at the starting.

Step 4 : Set the iteration count $IT = 0$

Step 5 : Set the input pattern count $IP = 1$

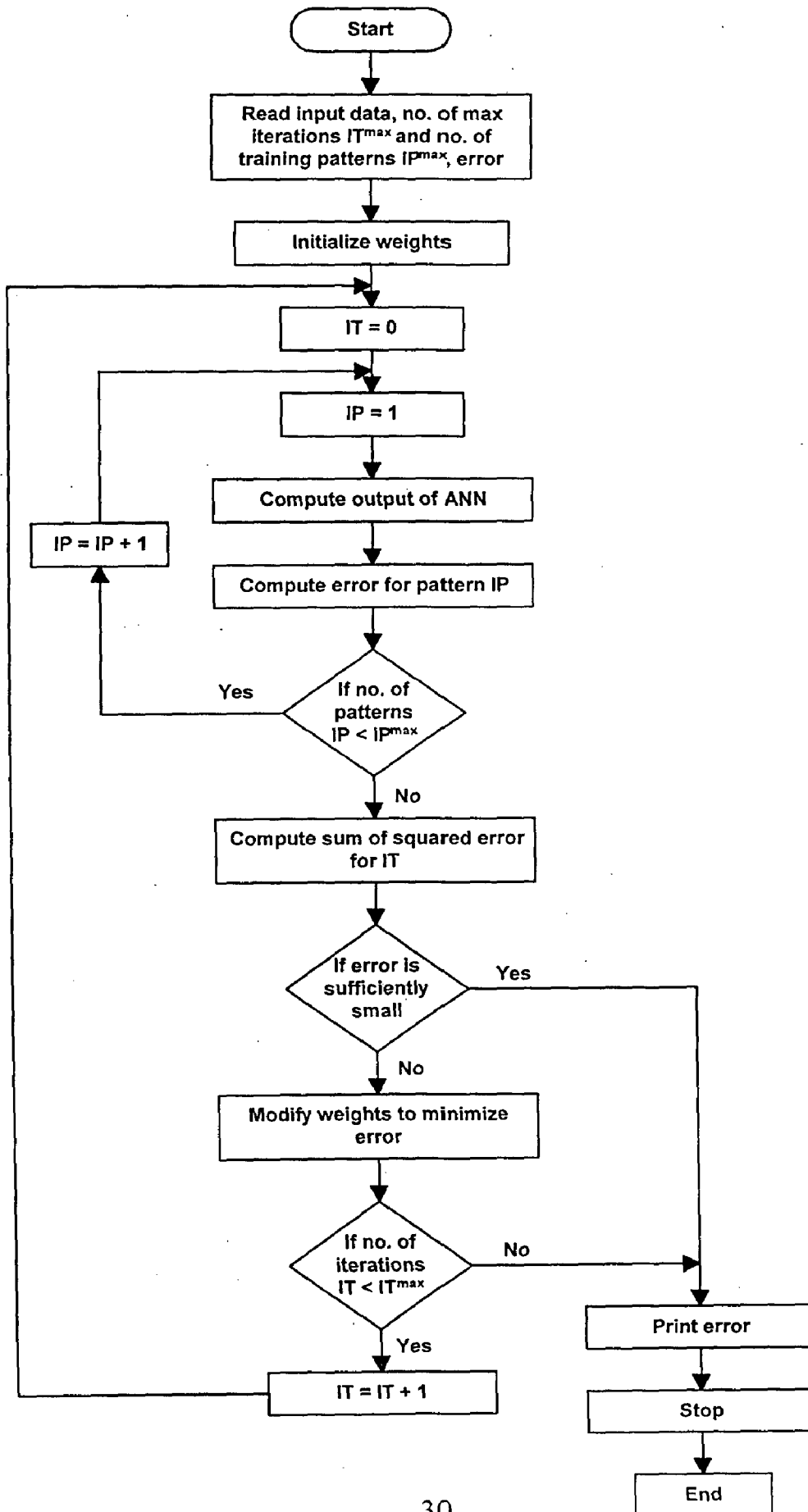
Step 6 : Calculate the output of ANN and compute the error.

Step 7 : If the number of patterns are less than IP^{\max} ,, then increment the $IP = IP + 1$, otherwise go to next step.

Step 8 : Check for the error sufficiency. If the error is less than desired, stop the processes, otherwise modify the weights.

Step 9 : Check the number of iterations. If the iteration are less than IT^{\max} , then increment the IT to $IT = IT + 1$ and go to the step 5, otherwise stop the processes.

3.4 FLOWCHART FOR TRAINING OF BACK-PROPAGATION ALGORITHM



Chapter 4

RESULTS AND DISCUSSIONS

4.1 NEURAL NETWORK TRAINING PROCESS

A feature encountered in applying neural networks to estimating harmonic current sources was the separability of input-output pairs. When harmonic source measurements (which are neural network outputs) were paired with the input measurements (which consists of fundamental load currents and bus voltages at all non-linear load buses as well as available permanent harmonic line current measurements), it was found [23] that each quantity in the output (real and imaginary parts of each harmonic) was relatively independent. This would be expected for harmonic sources with varying firing angles and/or magnitude. The output corresponding to particular harmonic source would be sensitive only to a particular subset of hidden layer. It was therefore advantageous to divide the neural network into separate networks for each known harmonic source. These can be further subdivided into two separate neural networks representing real and imaginary parts of the harmonic current source, which also behaves independently. This eliminates the need to adjust a large number of weights interconnecting the hidden layer with most of the outputs essentially to zero, which aided in obtaining convergence during the training sessions.

The structured neural network of figure shown in Fig. 4.1 is divided into multiple parallel-networks as mentioned above, all with the same inputs, but each with a single output (real value). The input set consists of real numbers representing the real and imaginary parts of fundamental load currents and bus voltages at all non-linear load buses and the fundamental load currents and harmonic complex currents (corresponding to harmonic order of its output) at the permanent metering points in the lines. In the training process for the neural networks, the initial weights and thresholds were randomly selected. The other parameters in the training process were learning rate η , which is initially chosen to small (0.02) to prevent overshoot, and the momentum factor, β , which is set to 0.01 (constant).

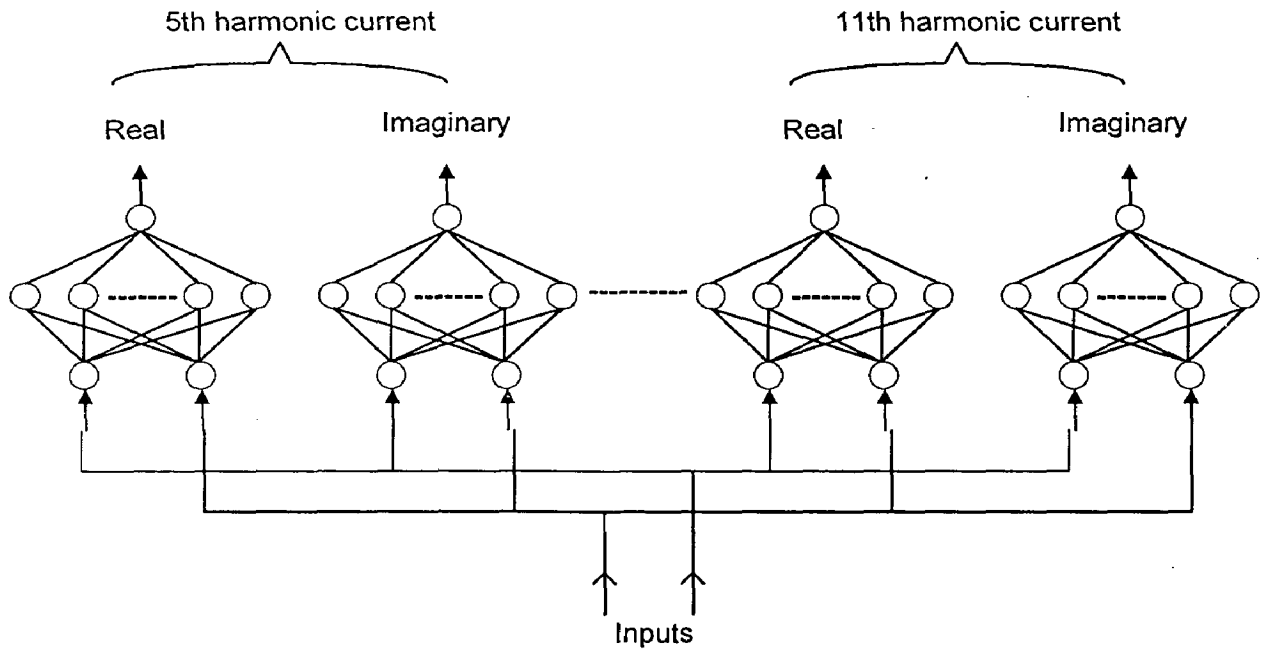


Figure 4.1 : Structured Neural Network

As the algorithm is converged, the learning rate was increased to accelerate the convergence. In cases where the algorithm did not converge, or the output converged to values different than the training output, the initial weights and thresholds were altered and the process was started again.

4.2 TRAINING OF 18 BUS SYSTEM

In the present work the above discussed training process was applied to 18 bus system taken from the reference [28] shown in Fig. 4.2. The 18 bus system consists of a nine linear loads and one non-linear load (converter load). For training the input set consists of a real and imaginary parts of load current and bus voltages at bus 5 and the fundamental and harmonic complex currents (corresponding to harmonic order of its output) at the permanently metering points on the lines 5-4 and 5-6, a total of 12 inputs. The outputs, each form a separate neural network are real numbers which represents the real and imaginary parts of 5th, 7th and 11th harmonics injected at bus 5. A total of 6 networks for identifying 5th, 7th and 11th harmonics were trained, in addition to input and output layer, each network contains a 30 node hidden layer.

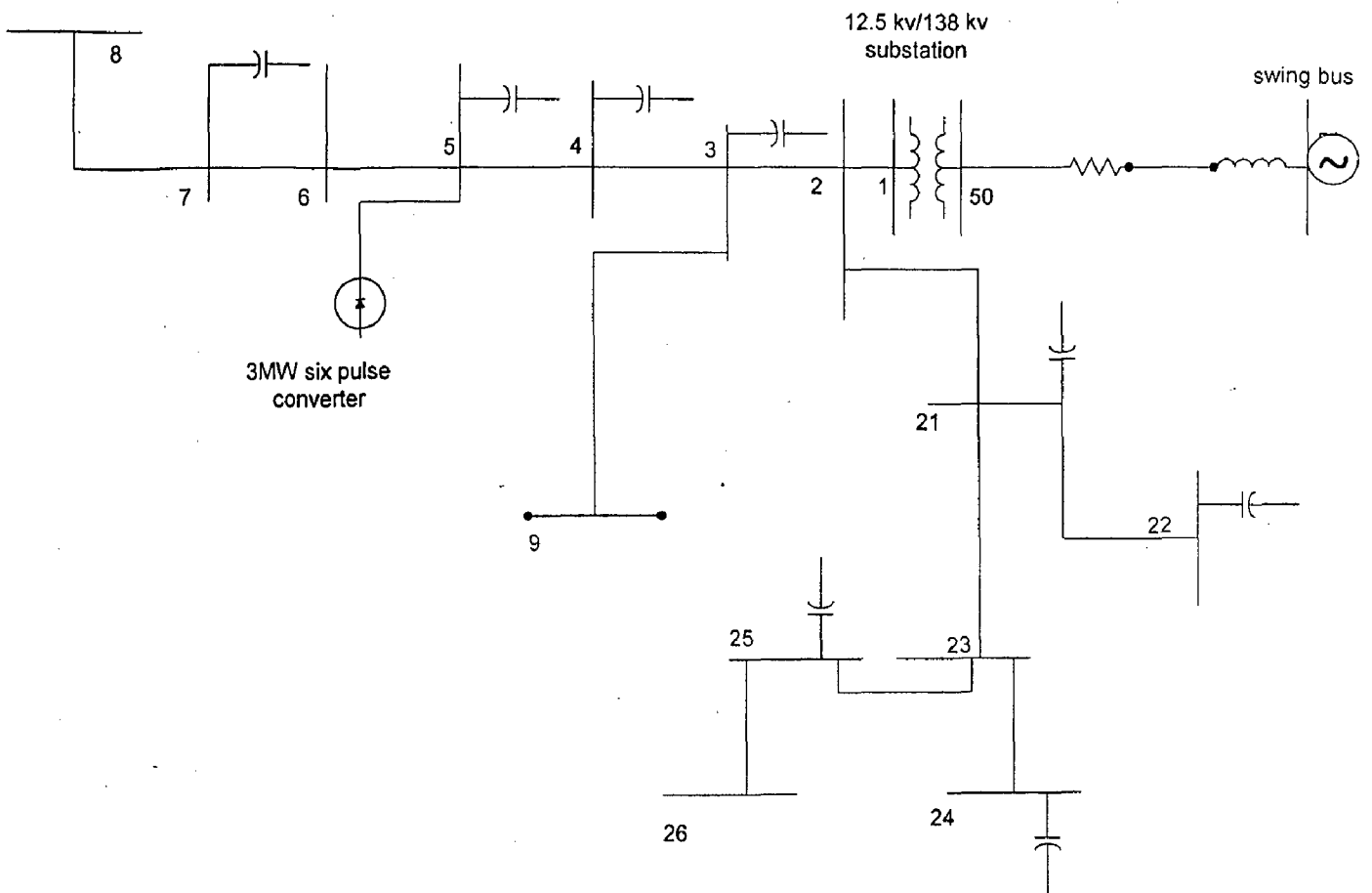


Figure 4.2 : 18 bus example system

The neural networks were trained with a series of 70 input-output pairs obtained by varying the non-linear load at bus 5 in the range from -20% to $+20\%$ of the "base" load. During the training the learning parameter $\eta = 0.2$ is used to achieve the convergence. In case of 5th harmonic the rms error obtained during the training was 0.001, for 7th harmonic 0.03 and for 11th harmonic 0.005. During training the ANN it has been observed that with the increase of order of harmonics, the convergence becomes difficult and time consuming. After the neural networks were trained, it was tested by two simulation studies. It has been done by varying the load at non-linear load bus in between the same ranges (-20% to 20%) that have been used for training. The results of the two tests are shown in Tables 4.1 and 4.2 respectively.

Table 4.1 : Results of Test-1

All the values are in P.U.

Harmonic currents Outputs	5 th harmonic current		7 th harmonic current		11 th harmonic current	
	Real part	Imagina ry part	Real part	Imagina ry part	Real part	Imagina ry part
Desired output	0.04525 8	0.061623	- 0.037726	- 0.039478	0.025326	0.006172
Neural network output	0.04496 8	0.062086	- 0.038346	- 0.039897	0.025608	0.005988

Table 4.2 : Results of Test-2

Harmonic currents Outputs	5 th harmonic current		7 th harmonic current		11 th harmonic current	
	Real part	Imagina ry part	Real part	Imagina ry part	Real part	Imagina ry part
Desired output	- 0.056855	0.05264 8	0.052986	- 0.015999	- 0.025207	- 0.007899
Neural network output	- 0.056084	0.05134 8	0.052089	- 0.016877	- 0.024968	- 0.008182

Chapter – 5

Conclusions and scope for future work

Conclusions

Conventional methods for predicting harmonics in power system are less accurate and time consuming. Artificial Neural Network (ANN) based methods accurately give estimates during testing once they are successfully trained and they give results with in short time. The following points concluded from this study.

- (i) The conventional Newton-Raphson power flow method has been modified by including current and apparent volt-ampere balance and there by permits harmonic power flow studies.
- (ii) A method to determine low audio range power system harmonics related by line commutated converters and non-linear loads has been described.
- (iii) An artificial Neural-Network based method has been presented for predicting harmonics currents in power system. A three-layered feed forward structured neural network was constructed with backpropagation learning algorithm.
- (iv) ANN was trained and tested with an example system. The results obtained from the simulation studies showed acceptable estimates.
- (v) During training of ANN, it was observed that with increase of the order of harmonics the convergence becomes difficult and time consuming.

Scope for future work

In the present study, an example system taken for training and testing of a neural network consists of one non-linear load (converter load). In the future, this work can be extended to consider the system which consists of multiple non-linear loads for estimating and analyzing the severity of the problem.

REFERENCES

1. Szabados, B., "On the Interaction between Power System Configuration and Industrial Rectifier Harmonic Interference", IEEE Trans. PAS-100, No. 8, August 1982, pp. 2762-2769.
2. Pilleggi, D.J., Chandra, N.H. and Emanuel, A. E., "Prediction of Harmonic Voltages in Distribution System", IEEE Trans. PAS-100, No. 6, 1981, pp. 1307-1315.
3. Mahmoud, A.A., and Schultz, R.D., "A Method for Analysing Harmonic Distribution in AC Power System", IEEE Trans. PAS-101, No. 6, June 1982, pp. 1815-1824.
4. Arrillaga, J., Densem, T.J., and Harker, B.J., "Zero Sequence Harmonic Current Generation in Transmission Lines Connected to Large Converter Plant", IEEE Trans PAS-102, No. 7, July 1983, pp. 2357-2363.
5. Arrilaga, J., Bodger, P.S. and Densem, T.J., "3- ϕ Transmission System Modelling for Harmonic Penetration Studies", IEEE Trans. PAS-103, No. 2, Feb. 1984, pp. 310-317.
6. Acha, E. and Arrillaga, J., "Harmonic Norton Equivalent for the Magnetising Branch of a Transformer", IEEE Proc., Vol. 134, Pt. C, No. 2, March 1987, pp. 162-169.
7. Semlysen, A. and Eggleston, J.F. "Admittance Model of a Synchronous Machine for Harmonic Analysis", IEEE Trans. on PS, Vol. 2, No. 4, November 1987, pp. 833-839.
8. Carpinelli, G., Gagligardi, F., Ruso, M. and Villacci, D., "Generalised Converter Models for Iterative Harmonic Analysis in Power Systems", IEE Proc., Vol. 141, Pt. C, No. 5, Sept., 1994, pp. 445-451.
9. Heydt, G.T. and Xia, D., "Harmonic Power Flow Studies Part I and Part II", IEEE Trans PAS-101, No. 6, June 1982, pp. 1257-1270.
10. Grady, W.M. and Heydt, G.T., "Prediction of Power System Harmonics Due to Gaseous Discharge Lighting", IEEE Trans. PAS-104, No. 7, March 1985, pp. 554-561.

11. Tamby, J.P. and John, V.I., "Q'HARM – A Harmonic Power Flow Programme for Small Power Systems", IEEE Trans. on PS, Vol. 3, No. 3, August 1988, pp. 949-955.
12. Hyedt, G.T., "Identification of Harmonic Sources by a State Estimation Technique", IEEE Trans. on PWRD, Vol. 4, No. 1, January 1989, pp. 5690576.
13. Xu, W., Marti, J. and Dommel, H.W., "Multiphase Harmonic Load Flow Solution Technique", IEEE Trans. on PS, Vol. 6, No. 1, Feb. 1991, pp. 174-182.
14. Girggis, A.A., Binchang, W. and Markram, E.B., "A Digital Recursive Measurement Scheme for Online Tracking of Power System Harmonics", IEEE Trans. on PWRD, Vol. 6, No. 3, July 1991, pp. 1153-1160.
15. Vinay Sharma, Fleming, R.T., and Nickamy Leo, "An Iterative Approach for Analysis of Harmonic Penetration in the Power Transmission Networks", IEEE Trans. on PWRD, Vol. 6, No. 3, 1991.
16. Valcarcel, N. and Mayordomo, J. G., "Harmonic Power Flow for Unbalanced Systems", IEEE Trans. on PWRD, Vol. 8, No. 4, October 1993.
17. Carbone, R., Fantauzzi, M. and Galiardi, F., "Some Constraints on the Iterative Harmonic Analysis Convergence", IEEE Trans. on PWRD, Vol. 8, No. 2, April 1993, pp. 487-493.
18. Caramia, P., Carpinelli, G., Rossi, F. and Verde, P., "A Probabilistic Method for Harmonic Analysis", IEEE Proc., Vol. 141, No. 2, 1994.
19. Arrillaga, J., Medina, A. and Kisboa, M.A., "The Harmonic Domain, A Frame of Reference for Power System Harmonic Analysis", IEEE Trans. on PS, Vol. 10, No. 1, Feb. 1995.
20. Arrillaga, J., Watson, N.R. and Callaghan, C.D., "3 Phase AC-DC Load and Harmonic Flows", IEEE Trans on PWRD, Vol. 6, No. 1, 1991, pp. 238-244.
21. Song, W., Grady, W.M. and Heydt, G.T., "The Integration of HVDC Subsystem into the Harmonic Power Flow Algorithm", IEEE Trans. PAS-103, No. 8, Aug. 1984, pp. 1953-1961.
22. Smith, B.C., Watson, N.R., Wood, A.R., and Arrillaga, J., "A Newton Solution for the Harmonic Phasor Analysis of AC/DC Converter", IEEE Trans. on PS, Vol. 11, No. 2, April 1996.

23. Widrow, B. and Lehr, M.A., "30 Years of Adaptive Neural Networks : Perceptrons, Madalinic and Backpropagation", Proc. IEEE, Vol. 78, 1990, pp. 1415-1442.
24. Hartana, R.K., and Richards, G.G., "Harmonic Source Monitoring and Identification Using Neural Networks", IEEE Trans. on PS, Vol. 5, No. 4, November 1990, pp. 1098-1104.
25. Mori, H., Itou, K. and Uematsu, H., "An Artificial Neural Network Based Method for Predicting Power System Voltage Harmonics", IEEE Trans. on PWRD, Vol. 7, No. 1, January 1992, pp. 402-409.
26. Dash, P.K., Swain, D.P. and Liew, A.C., "An Adaptive Linear Combiner for On-line Tracking of Power System Harmonics", IEEE Trans. on PS, Vol. 11, No. 4, November 1996, pp. 1730-1735.
27. Arrilegga, J., Bradley and Bodger, P.S., "Power System Harmonics", John Wiley, 1985.
28. Grady, W.M., and Samotyi, M.J., "The Application of Network Objective Function for Actively Minimizing the Impact of Voltage Harmonics in Power Systems", IEEE Trans on PWRD, Vol. 7, No. 3, July 1992, pp. 1379-1386.
29. Griffin, J., "Fluorescent Lamps, Neutral Currents and Standby Generators", Electrical Review, Vol. 204, No. 2, pp. 21-22, January 12, 1979.
30. Zurada, J. M., "Introduction to Artificial Neural Systems", Wast Publications 1994.

Appendix A

Table A-1. Bus Data

Bus Num	Bus Name	Bus Type	P Gen (%)	Q Gen (%)	S VA (%)	P Load (%)	Q Load (%)	Bus Volt (%)	Shunt Load (%)
1	garl2.5	03	0.0	0.0	0.0	0.0	0.0	0.0	0.0
2	cap1-2	03	0.0	0.0	0.0	2.0	1.2	0.0	-10.5
3	cap4	03	0.0	0.0	0.0	4.0	2.5	0.0	-6.0
4	cap3	03	0.0	0.0	0.0	15.0	9.3	0.0	-6.0
5	sixpulse	23	0.0	0.0	0.0	30.0	22.6	0.0	-18.0
6	six	03	0.0	0.0	0.0	8.0	5.0	0.0	0.0
7	cap6	03	0.0	0.0	0.0	2.0	1.2	0.0	-6.0
8	eight	03	0.0	0.0	0.0	10.0	6.2	0.0	0.0
9	nine	03	0.0	0.0	0.0	5.0	3.1	0.0	0.0
20	cap7	03	0.0	0.0	0.0	10.0	6.2	0.0	-6.0
21	cap8-9	03	0.0	0.0	0.0	3.0	1.9	0.0	-12.0
22	bus22	03	0.0	0.0	0.0	2.0	1.2	0.0	0.0
23	bus23	03	0.0	0.0	0.0	8.0	5.0	0.0	0.0
24	cap10-11	03	0.0	0.0	0.0	5.0	3.1	0.0	-15.0
25	cap12	03	0.0	0.0	0.0	10.0	6.2	0.0	-9.0
26	bus26	03	0.0	0.0	0.0	2.0	1.2	0.0	0.0
50	garl38	03	0.0	0.0	0.0	0.0	0.0	0.0	-12.0
51	swing	01	0.0	0.0	0.0	0.0	0.0	105.0	0.0

Table A-2.Line Data

Bus to	Bus from	R(t) (%)	X(t) (%)	Line Chag (%)	Length (mi)
1	2	0.431	1.204	0.0035	0.318
2	3	0.601	1.677	0.0049	0.443
3	4	0.316	0.882	0.0020	0.233
4	5	0.896	2.502	0.0073	0.661
5	6	0.295	0.824	0.0024	0.218
6	7	1.720	2.120	0.0046	0.455
7	8	4.070	3.053	0.0051	0.568
2	9	1.706	2.209	0.0043	0.451
1	20	2.910	3.768	0.0074	0.769
20	21	2.222	2.877	0.0056	0.587
21	22	4.503	6.218	0.0122	1.269
21	23	3.985	5.160	0.0101	1.053
23	24	2.910	3.768	0.0074	0.769
23	25	3.727	4.593	0.0100	0.985
25	26	2.208	2.720	0.0059	0.583
50	1	0.312	6.753	0.000	0.000
50	51	0.050	0.344	0.000	0.000
51	0	0.000	0.010	0.000	0.000

Fourier Expansion of Phase Currents at Non-Linear Load Busses

With reference to Fig (2.4) in chapter 2 , The transformer secondary line to neutral voltages be $u_a(t)$, $u_b(t)$, $u_c(t)$ with fourier series.

$$u_a(t) = \sum_k u_k \sin(k\omega_0 t + \phi'_k)$$

$$u_b(t) = \sum_k u_k \sin(k\omega_0(t - \frac{T_0}{3}) + \phi'_k)$$

$$= \sum_k u_k \sin(k\omega_0 t + \phi'_k - \frac{2\pi\delta_k}{3})$$

$$u_c(t) = \sum_k u_k \sin(k\omega_0 t + \phi'_k + \frac{2\pi\delta_k}{3})$$

Where T_0 is the period of ω_0 , ω_0 is the fundamental frequency , u_k are the per unit fourier coefficients,

$$\begin{aligned} \delta_k &= 1 & k=1,4,7,\dots \\ &= -1 & k=2,5,8,\dots \\ &= 0 & k=3,6,9,\dots \end{aligned}$$

and \sum_k denotes summation $k=1$ to ∞ .Note that $T_0 = (2\pi)/\omega_0$. Examination of equations (A1-A4) shows that the line to neutral voltages are positive sequence voltages for $k=1,4,7,\dots$, negative sequence only for $k=2,5,8,\dots$ and zero sequence for $k=3,6,9,\dots$

The line to line voltages are $u_{ab}(t)$, $u_{ca}(t)$ and $u_{bc}(t)$ are given in per unit as

$$u_{ab}(t) = u_a(t) - u_b(t) = \sum_k u_k \sin(k\omega_0 t + \phi'_k)$$

$$u_{bc}(t) = u_b(t) - u_c(t) = \sum_k u_k \sin(k\omega_0 t + \phi'_k - \frac{2\pi\delta_k}{3})$$

$$u_{ca}(t) = u_c(t) - u_a(t) = \sum_k u_k \sin(k\omega_0 t + \phi_k + \frac{2\pi\delta_k}{3})$$

Where

$$\phi_k = \phi'_k + \delta_k \frac{\pi}{6}$$

These transformer secondary line to line terminal voltages do not contain any third harmonic(k=3). Independent of the transformer connection since when k=3, u_a, u_b, u_c are only in zero sequence, which cannot be applied to the bridge rectifier. Similar examination shows that for line to line voltages, only +ve sequences occur for k=1,4,7... and only -ve sequences occur for k=2,5,8 .. No components exist for k=3,6,9. The line to line voltages shifted by $\delta_k (\pi/6)$ from the line to neutral voltages.

There is further considerable simplification for bridge rectifier since no even harmonics exist in either line voltages or currents. This is the case since u_{ab}, u_{bc}, u_{ca} are odd functions,

$$u_{ab}(t \pm \frac{T_0}{2}) = -u_{ab}(t) = u_{ba}(t)$$

Since no even harmonic voltages occur, no even harmonic currents will flow in the network. From fig B1, let α be the rectifier triggering angle. Consider only $u_{ab}(t)$ (the other line to neutral voltages are $\pm\pi/3$ phase shifted): the period $\alpha < t < \alpha + \mu/3$ is divided into a commutation period $\alpha < t < \alpha + \mu$ and a conduction period $\alpha + \mu < t < \alpha + \mu/3$. In these periods, it is desired to write and solve the Kirchoff's law equations for voltage and current. The result is used to obtain the Fourier analysis of the rectifier supply voltage. For the commutation period u_{cb} and u_{ab} are applied conducting SCR's $c_1, a_1,$ and b_2 .

$$Lp i_a^{(1)} - Lp i_c^{(1)} = u_{ab}(t) - u_{cb}(t) \quad (B12)$$

$$(R + (2L + F)p)i_a^{(1)} + (R + (L + F)p)i_c^{(1)} = u_{ab}(t) - E \quad (B13)$$

$$p \equiv \frac{d}{dt} \quad (B14)$$

The subscript (1) denotes the first period of interest. Figure (B2) will help for the understanding of this period. Solving for $i_a^{(1)}$, $i_b^{(1)}$, and $i_c^{(1)}$ yields

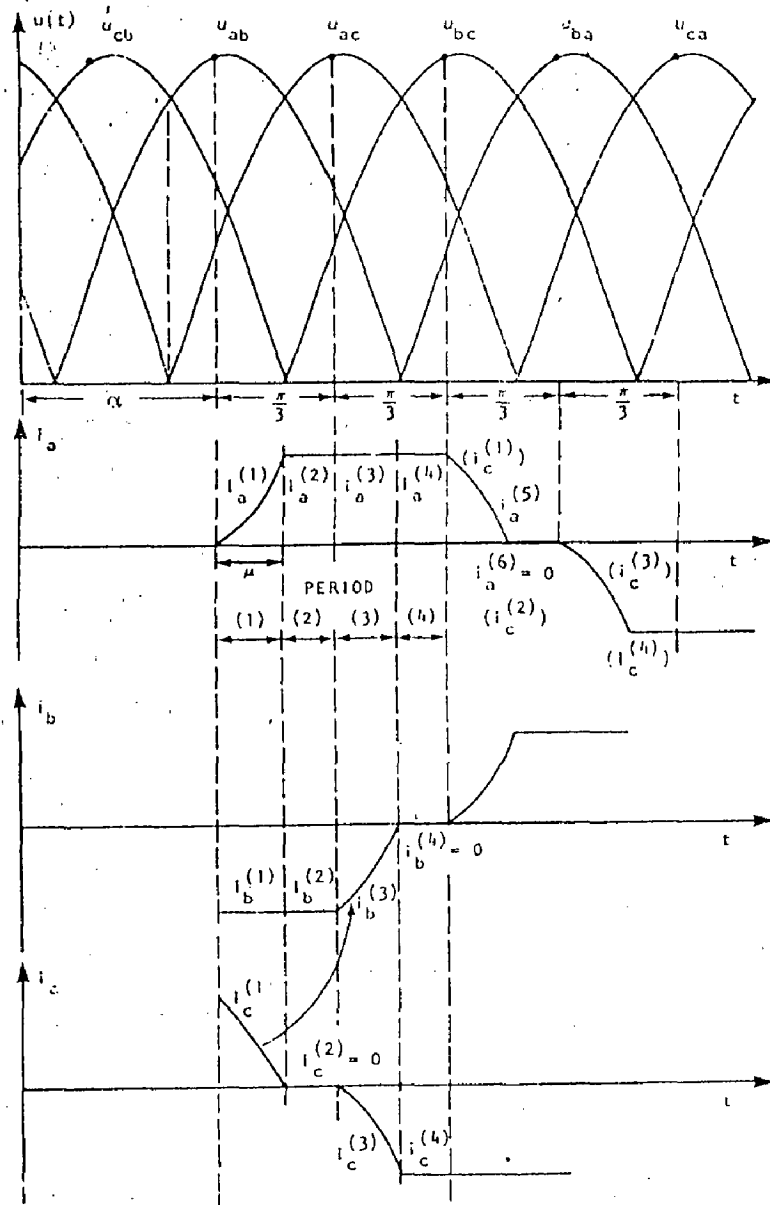


Figure B1 Phase Currents in a Bridge Rectifier

$$i_a^{(1)}(t) = K_1^{(1)} + K_2^{(1)}e^{p_1 t} + f_1^{(1)}(u_k, t) - \frac{E}{2R} \quad (B15)$$

$$i_c^{(1)}(t) = -K_1^{(1)} + K_2^{(1)}e^{p_1 t} + f_c^{(1)}(u_k, t) - \frac{E}{2R} \quad (B16)$$

$$i_b^{(1)}(t) = -i_a^{(1)}(t) - i_c^{(1)}(t) \quad (B17)$$

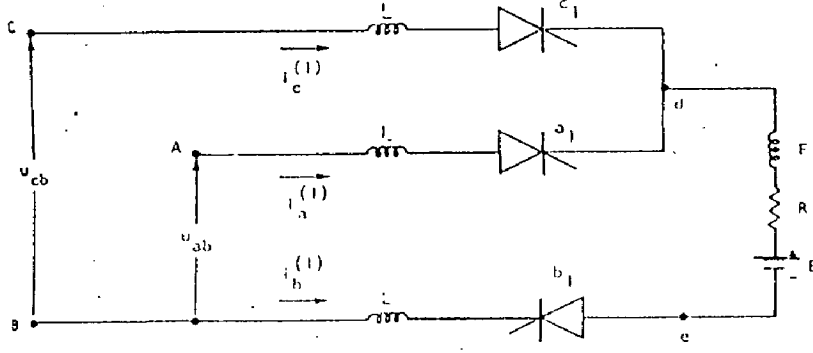


Figure B2 First Case Studied

where

$$f_a^{(1)}(u_{k,t}) = \sum_{k=1,5,7,11} \frac{u_k}{z_{k1}} \sin(k\omega_0 t + \phi_k - \theta_{k1}) - \sum_{k=1,5,7,11} \frac{u_k^2 k_2}{z_{k1} z_{k3}} \sin(k\omega_0 t + \phi_k + \theta_{k2} - \theta_{k1} - \frac{\pi}{2} + \frac{2\pi\delta_k}{3}) \quad (B18)$$

$$f_c^{(1)}(u_{k,t}) = \sum_{k=1,5,7,11} \frac{u_k}{z_{k1}} \sin(k\omega_0 t + \phi_k - \theta_{k1}) - \sum_{k=1,5,7,11} \frac{u_k^2 k_4}{z_{k1} z_{k3}} \sin(k\omega_0 t + \phi_k + \theta_{k4} - \theta_{k1} - \frac{\pi}{2} + \frac{2\pi\delta_k}{3}) \quad (B19)$$

and the $K^{(1)}$ terms are constants which are determined by initial conditions and continuity expressions, and

$$z_{k1} \text{Arg}(\theta_{k1}) = 2R + j(3L + 2F)k \quad (B20)$$

$$z_{k2} \text{Arg}(\theta_{k2}) = R + j(L + F)k \quad (B21)$$

$$z_{k3} \text{Arg}(\frac{\pi}{2}) = jLk \quad (B22)$$

$$z_{k4} \text{Arg}(\theta_{k4}) = R + j(2L + F)k \quad (B23)$$

$$P_1 = \frac{-2R}{3L + 2F} \quad (B24)$$

and (A) Arg (B) denoted a vector of length A and phase angle B (radians).

Continuity at $t = \alpha$ gives Eqs. (B25-B26)

$$0 = i_a^{(1)}(\alpha) = K_1^{(1)} + K_2^{(1)} e^{P_1 \alpha} + f_a^{(1)}(u_k, \alpha) - \frac{E}{2R} \quad (B25)$$

$$i_c^{(1)}(\alpha) = i_c^{(1)}(\alpha^-) = -K_1^{(1)} + K_2^{(1)} e^{p_1 \alpha} + f_c^{(1)}(u_k, \alpha) - \frac{E}{2R} \quad (\text{B26})$$

The commutation period ends at $t = \alpha + \mu$, $\mu < \pi/3$. The commutation angle μ is solved from $i_c^{(1)}(\alpha + \mu) = 0$ in Eq. (B16).

The second period, $\alpha + \mu \leq t \leq \alpha + \pi/3$ is solved similarly. Figure B3 refers to this period and SCR's a_1 , b_2 are conducting. The defining differential equation is (B27) and the solution is (B28-B30) (note the use of the superscript (2) to denote the second period of interest),

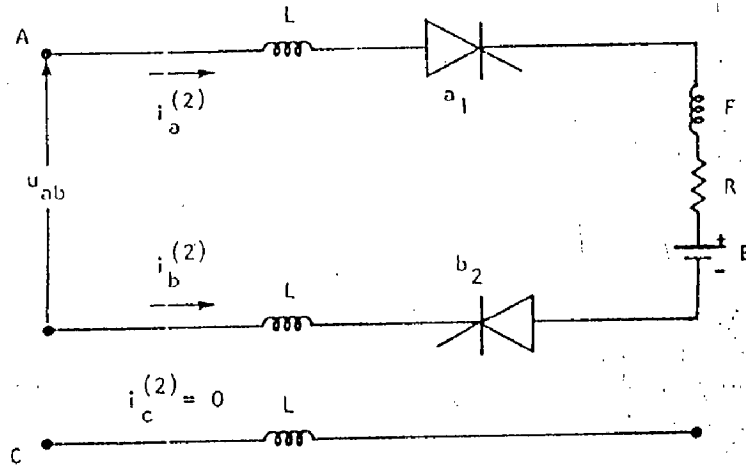


Figure B3 Second Case Studied

$$u_{ab}(t) - E = i_a^{(2)}(R + (2L + F)_p) \quad (\text{B27})$$

$$i_a^{(2)}(t) = K_2^{(2)} e^{p_2 t} + f_a^{(2)}(u_k, t) - \frac{E}{R} \quad (\text{B28})$$

$$i_b^{(2)}(t) = -i_a^{(2)} \quad (\text{B29})$$

$$i_c^{(2)}(t) = 0 \quad (\text{B30})$$

where

$$f_a^{(2)}(u_k, t) = \sum_{k=1,5,7,11,\dots} \frac{u_k}{Z_{k4}} \sin(k\omega_o t + \phi_k - \theta_{k4}) \quad (\text{B31})$$

$$P_2 = \frac{-R}{2L + F} \quad (\text{B31})$$

and $K_2^{(2)}$ is determined by the continuity of i_a at $t = \alpha + \mu$. Fig. (B4) refers to this period. The differential equations are

$$Lp i_b^{(3)} - Lp i_c^{(3)} = u_{ac} - u_{ab} \quad (B32)$$

$$-(R + (2L + F)p) i_c^{(3)} - (R + (L + Fp)) i_b^{(3)} = u_{ac} - E \quad (B33)$$

The initial condition is

$$i_c^{(3)}(\alpha + \pi/3) = 0 \quad (B34)$$

$$i_b^{(3)}(\alpha + \mu/3) = i_b^{(2)}(\alpha + \pi/3) \quad (B35)$$

and the solution is similar to the solution for $i_a^{(1)}$, $i_b^{(1)}$, $i_c^{(1)}$. Using the fact that the supply voltage in phase ac in the time current interval $(\alpha + \pi/3, \alpha + 2\pi/3)$ has the

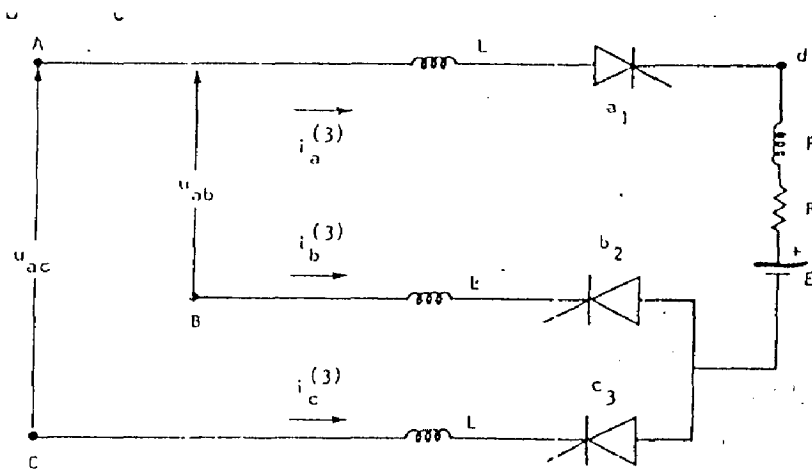


Figure B4 Third Case Studied

same value as that in phase ab for the interval $(a, \alpha + \pi/3)$, it is easy to show that

shifting $i_a^{(1)}$, $i_b^{(1)}$, $i_c^{(1)}$ by $\pi/3$ radians and reversing the sign results in $i_a^{(3)}$, $i_b^{(3)}$, $i_c^{(3)}$.

For example, in phase a,

$$\begin{aligned} i_a^{(3)}(t) &= -i_b^{(1)}(t - \pi/3) \\ &= 2K_2^{(1)} e^{p_1(t - \pi/3)} + f_a^{(1)}(u_k, t - \pi/3) + f_c^{(1)}(u_k, t - \pi/3) - E/R. \end{aligned}$$

Phase b and c are handled similarly.

After the commutation period, the situation of the phase a current is identical to that of the phase c current in $\alpha < t \leq \alpha + 2\pi/3$. In the time interval $\alpha + 4\pi/3 < t < \alpha + 2\pi$, the situation of i_a is identical to that of i_b in $\alpha < t < \alpha + 2\pi/3$.

The b and c currents are similarly related. Therefore for $\alpha + 2\pi/3 < t \leq \alpha + 4\pi/3$, $i_a(t)$ is found by shifting $i_c^{(1)}$ through $i_c^{(4)}$ by $2\pi/3$. For $\alpha + 4\pi/3 < t < \alpha + 2\pi$, i_a is found by shifting $i_b^{(1)}$ through $i_b^{(4)}$ by $4\pi/3$.

Hence

$$i_a(t) = -i_a(t + \pi)$$

and only odd harmonics exist in i_a provided that only odd harmonics exist in the supply voltage.

A Method for Calculating the Phase Currents of a Full Wave Bridge Loaded with And E-R-L Load

This Appendix concludes with final comments on the full wave bridge loaded as in Fig. A1. Two cases occur : When commutation does no exist, $i_a(t)$ is solved as indicated in the previous section where $K_2^{(2)}$ is obtained using initial conditions, $\mu = 0$, and $i_a^{(2)}(\alpha) = 0$. Then

$$i_a^{(2)}(\alpha) = K_2^{(2)} e^{p_2\alpha} + f_a^{(2)}(u_k, \alpha) = 0$$

and $K_2^{(2)}$ is found. Having found $i_a^{(2)}$, $i_b^{(2)}$ is also found ($i_b^{(2)} = -i_a^{(2)}$). Since the phase current cannot be negative in this period, the sign of i_a is checked at $t = \alpha + \pi/3$. If $i_a(\alpha + \pi/3)$ is zero, the period ends precisely at $t = \alpha + \pi/3$. If i_a is negative, this period has not ended at $\alpha + \pi/3$ and the ending time must be calculated (denote this ending time as t_1). Then t_1 is found from

$$i_a^{(2)}(t_1) = K_2^{(2)} e^{p_2 t_1} + f_a^{(2)}(u_k, t_1) - \frac{E}{R} = 0$$

If i_a is positive, the commutation period does not exist. This is the second case mentioned above and discussed next.

If the commutation period does not exist, the problem is more complex and the solution is briefly outlined here. In this case, the initial value of $i_c^{(1)}$ must be known to obtain $K_1^{(1)}$ and $K_2^{(1)}$. This problem is solved by noting

$$i_b^{(3)}(\alpha + \pi/3) = -i_c^{(1)}(\alpha)$$

$$i_b^{(3)}(\alpha + \pi/3) = i_b^{(2)}(\alpha + \pi/3)$$

$$i_b^{(2)}(\alpha + \pi/3) = -K_2^{(2)} e^{p_2(\alpha + \pi/3)} - f_a^{(2)}(u_k, \alpha + \pi/3) + \frac{E}{R}$$

Substitution of $i_b^{(2)}$ into Eq. (A14-A15) gives $K_1^{(1)}$, $K_2^{(1)}$ and $K_2^{(2)}$.

Unfortunately, the simultaneous solution of these constants requires the use of Newton's method since the simultaneous relations are transcendental. The result is summarised by introducing simplifying notation,

$$K_1 = K_1^{(1)}$$

$$K_2 = K_2^{(1)} e^{p_1 \alpha}$$

$$K_3 = K_2^{(2)} e^{p_2 \alpha}$$

$$A = \frac{E}{2R} - f_a^{(1)}(u_k, \alpha)$$

$$B = f_a^{(2)}(u_k, \alpha + \pi/3) - f_c^{(1)}(u_k, \alpha) - \frac{E}{2R}$$

$$D = -e^{p_2 \pi/3}$$

$$G = B - A - \frac{E}{R}$$

$$C = A + B$$

$$H_1 = e^{p_1 \mu} \quad H_2 = e^{p_2 \mu}$$

Then Newton's method is used as follows (after eliminating $K_1^{(1)}$ and $K_2^{(1)}$),

$$\begin{bmatrix} k_3 \\ \mu \end{bmatrix}_{\text{iteration } k+1} = \begin{bmatrix} k_3 \\ \mu \end{bmatrix}_{\text{iteration } k} + \Delta$$

$$\Delta = \begin{bmatrix} \frac{\partial F_1}{\partial K_3} & \frac{\partial F_1}{\partial \mu} \\ \frac{\partial F_2}{\partial K_3} & \frac{\partial F_2}{\partial \mu} \end{bmatrix} \begin{bmatrix} F_1(K_3, \mu) \\ F_2(K_3, \mu) \end{bmatrix}$$

The b and c currents are similarly related. Therefore for $\alpha + 2\pi/3 < t \leq \alpha + 4\pi/3$, $i_a(t)$ is found by shifting $i_c^{(1)}$ through $i_c^{(4)}$ by $2\pi/3$. For $\alpha + 4\pi/3 < t < \alpha + 2\pi$, i_a is found by shifting $i_b^{(1)}$ through $i_b^{(4)}$ by $4\pi/3$.

Hence

$$i_a(t) = -i_a(t + \pi)$$

and only odd harmonics exist in i_a provided that only odd harmonics exist in the supply voltage.

A Method for Calculating the Phase Currents of a Full Wave Bridge Loaded with And E-R-L Load

This Appendix concludes with final comments on the full wave bridge loaded as in Fig. A1. Two cases occur : When commutation does no exist, $i_a(t)$ is solved as indicated in the previous section where $K_2^{(2)}$ is obtained using initial conditions, $\mu = 0$, and $i_a^{(2)}(\alpha) = 0$. Then

$$i_a^{(2)}(\alpha) = K_2^{(2)} e^{p_2\alpha} + f_a^{(2)}(u_k, \alpha) = 0$$

and $K_2^{(2)}$ is found. Having found $i_a^{(2)}$, $i_b^{(2)}$ is also found ($i_b^{(2)} = -i_a^{(2)}$). Since the phase current cannot be negative in this period, the sign of i_a is checked at $t = \alpha + \pi/3$. If $i_a(\alpha + \pi/3)$ is zero, the period ends precisely at $t = \alpha + \pi/3$. If i_a is negative, this period has not ended at $\alpha + \pi/3$ and the ending time must be calculated (denote this ending time as t_1). Then t_1 is found from

$$i_a^{(2)}(t_1) = K_2^{(2)} e^{p_2 t_1} + f_a^{(2)}(u_k, t_1) - \frac{E}{R} = 0$$

If i_a is positive, the commutation period does not exist. This is the second case mentioned above and discussed next.

If the commutation period does not exist, the problem is more complex and the solution is briefly outlined here. In this case, the initial value of $i_c^{(1)}$ must be known to obtain $K_1^{(1)}$ and $K_2^{(1)}$. This problem is solved by noting

$$\frac{\partial F_1}{\partial K_3} = D - H_2$$

$$\frac{\partial F_2}{\partial K_3} = -(H_2 + DH_1)$$

$$\frac{\partial F_1}{\partial \mu} = -p_2 H_2 K_3 + f_1(\alpha + \mu)$$

$$\frac{\partial F_2}{\partial \mu} = -(p_2 H_2 + Dp_1 H_1) K_3 + p_1 C H_1 + f_2(\alpha + \mu)$$

Also

$$F_1(k_3 + \mu) = (D - H_2)K_3 + f_1(\alpha + \mu) - G$$

$$F_2(k_3 + \mu) = -(H_2 + DH_1)K_3 + f_2(\alpha + \mu) + CH_1$$

$$f_1(\alpha + \mu) = f_a^{(1)}(\mu_k + \alpha + \mu) - f_c^{(1)}(u_k, \alpha + \mu) - f_a^{(2)}(u_k, \alpha + \mu)$$

$$f_2(\alpha + \mu) = f_a^{(1)}(\mu_k + \alpha + \mu) - f_c^{(1)}(u_k, \alpha + \mu) - f_a^{(2)}(u_k, \alpha + \mu)$$

After obtaining K_3 and μ , K_1 and K_2 are calculated from

$$K_1 = K_2 + A$$

$$2K_2 + DK_3 = C$$